CIRCADIAN REGULATION OF GENE EXPRESSION IN THE ELECTRIC ORGAN OF THE GYMNOTIFORM FISH *BRACHYHYPOPOMUS GAUDERIO*

by

Shann E. Cox

Thesis submitted in partial fulfillment of the requirements for the Degree of
Bachelor of Science
with Honours in Biology

Cape Breton University

May 2024

This thesis by Shann E. Cox

is accepted in its present form by the

Department of Biology

as satisfying the thesis requirements for the degree of

Bachelor of Science with Honours

Approved by the Thesis Supervisor

_____ _____

(*Dr. Vielka L. Salazar*) Date

Approved by Committee

_____ _____

(*Dr. Rod Beresford*) Date

_____ _____

(Dr. Timothy Rawlings) Date

Title: Circadian regulation of gene expression in the electric organ of the gymnotiform fish *Brachyhypopomus gauderio*.

A thesis submitted in partial fulfillment of the requirements for BIOL-4900 Honours Thesis in Biology, in the Department of Biology, Cape Breton University, Sydney, Nova Scotia, CANADA.

By: Shann E. Cox
May, 2024

Table of Contents

List of Tables

List of Figures

Figure 7. Log ratio (M) and mean average (A) plot of differently expressed genes. Average log CPM = average log2 counts per million; log-fold-change = expression changes between daytime and nighttime male *B. gauderio* samples. The two vertical lines indicate the up-down threshold for differential expressed genes. Values >1 represents an upregulation and <-1 represents a downregulation in nighttime gene expression relative to daytime values in A) males, and B) females *B. gauderio*.

Figure 8. Bar graph of the number of upregulated and down regulated genes determined in the nighttime relative to the daytime in *B. gauderio* A) males, and B) females.

Figure 9. Volcano plots depicting -log10(FDR) values against log2(FC) in A) males and B) females *B. gauderio*. Log2(FC) values > +1 and above the 0.1 threshold for –log10(FDR) (purple dots) are DEGs that are significantly upregulated in the nighttime compared to the daytime, while log2(FC) values < -1 and above the 0.1 threshold for –log10(FDR) (orange dots) are DEGs that are downregulated in the nighttime compared to the daytime. Log2(FC) values that are between -1 and 1 and below the 0.1 threshold for –log10(FDR) (grey points) represent no significant DEGs.

Figure 10. A schematic of the proposed cellular pathway linking the binding of IGF-II to the IGF receptor to trafficking of Na^+/K^+ ATPase pumps to the electrocyte membrane. The pathway suggests that the binding of IGF-II to the IGF receptor (IGFR) activates the insulin receptor substrate 1 protein (IRS1), which in turn activates phosphoinositide 3 kinase (PIK3), trafficking Na^+/K^+ ATPases to the electrocyte membrane. In my study the insulin receptor substrate 2 protein was upregulated (adapted from Gallant *et al*., 2014; Ivey, 2019).

Figure 11. A schematic of a proposed cellular pathway connecting IGF-II, Na^+/K^+ ATPase, SCN4Aa, and GLUT4 in their roles in EOD modulation. The pathway suggests that the binding of IGF-II to the IGF receptor (IGFR) activates intermediate signaling molecules which result in the trafficking of Na^+/K^+ ATPase to the electrocyte membrane to reset the membrane potential from the extra Na^+ ions. The Na^+/K^+ ATPases costs energy which can be offset by the transportation of GLUT4 into the membrane for glucose uptake (adapted from Gallant *et al*., 2014; Wang et al., 2020). Voltage-gated sodium channels in the electrocyte membrane are also shown in this figure to highlight their importance in the generation of the EOD.

List of Appendices

List of Abbreviations

ACTH, adrenocorticotropic hormone

α-MSH, alpha melanocyte stimulating hormone

AP, action potential

atp1a2a, sodium-potassium ATPase 2 alpha (catalytic subunit)

BMAL1, brain and muscle aren't-like 1

CLOCK, circadian locomotor output cycle kaput

CPM, counts per million

cry, cryptochrome gene

CRY, cryptochrome protein

DEGs, differentially expressed genes

EO, electric organ

EOD, electric organ discharge

FC, fold change

FDR, false discover rate

GLUT4, glucose transporter type 4

IGF-II, insulin-like growth factor 2

μEOD, microEOD

mRNA, messenger RNA

MC5R, melanocortin receptor 5

Na+/K+ ATPase, sodium-potassium ATPase

per, period gene

PER, period protein

PI3K, phosphoinositide 3 kinase

P1, phase 1

P2, phase 2

RMP, resting membrane potential

RPK, reads per kilobase

SCN, suprachiasmatic nucleus

scn4aa, sodium channel protein type 4 subunit alpha A gene

TPM, transcripts per million

ZNRF2a, zinc and ring finger protein 2a

Acknowledgements

I would like to thank my Honours supervisor, Dr. Vielka Salazar, for her continuous support and knowledge throughout the process of writing my thesis, as well as, for always pushing me out of my comfort zone which has enabled me to gain confidence in conducting research. Her passion and drive for research and her career does not go unnoticed and is truly inspiring. I would also like to thank her for hiring me to work in the Behavioural Neuroendocrinology Laboratory at Cape Breton University that has allowed me to pursue this project along with others during my time in the lab. I will also like to thank to my other two committee members Dr. Tim Rawlings and Dr. Rod Beresford for their valuable feedback and encouragement through my thesis project.

The work completed in this project would not have been possible without funding provided to Dr. Vielka Salazar from a NSERC Developing Discovery Grant (DDG) and CFI JLEF grants. I am also thankful for the funding that I received to gain the research skills and confidence that I needed to pursue an honours degree. These sources of funding include a Scotia Scholar Award from Research Nova Scotia, which allowed me to gain molecular biology skills this past summer leading into my thesis. I also have to thank past funding that I received to work in the Organic Chemistry lab, including a NSERC Undergraduate Student Research Award (USRA) and an Undergraduate Student Scholar Award (USSA). These opportunities commenced my passion for research.

Finally, I would like to thank my fellow Biology Honour students, especially Courtney Trask for her support throughout writing my thesis. I would also like to say a special thanks to Dr. Stephanie MacQuarrie who wasn't directly involved in my thesis but who encouraged me to get into research. This project would not have been possible without the encouragement and

support from my friends and family who always helped me when I was feeling overwhelmed and pushed me to keep going.

Abstract

Endogenous cellular circadian clocks have been shown to be major regulators of metabolic functions. The nocturnal gymnotiform fish *Brachyhypopomus gauderio* has emerged as a good candidate animal system to study the cellular and molecular mechanisms underlying the circadian regulation of energy metabolism. *B. gauderio* produce a weakly electric signal, referred to as an electric organ discharge (EOD), for habitat navigation and communication with conspecifics. The EOD displays sexual dimorphism, circadian regulation, and is highly energetically expensive. While both sexes of *B. gauderio* exhibit larger signals in the nighttime compared to the daytime, males exhibit a much larger signal increase in the nighttime. This enhanced nighttime EOD requires a large portion of a male's energy budget to EOD production. In addition, the EOD circadian change is mediated at the cellular level by hormones, such as melanocortins and androgens, and their effects on electrogenic membrane channels and transporters, such as voltage-gated sodium channels and sodium-potassium ATPases. However, genes associated with the link between the circadian rhythm and energy regulation have yet to be fully characterized in the electric organ of *B. gauderio*. For my Honours thesis project, I have used direct RNA sequencing to characterize the expression of genes in the electric organ from male (n=8) and female (n=4) *B. gauderio,* sampled during daytime and nighttime. When comparing nighttime to daytime, I found 231 upregulated genes and 108 down regulated genes in the EO of male *B. gauderio* samples, and 32 upregulated genes and 36 downregulated genes in the EO of female *B. gauderio*. Using a false discovery rate (FDR) statistical approach, I was able to identify significant differentially expressed genes in males, but not in females, and to categorize these genes into molecular mechanisms and regulatory pathways that may support males' EOD enhancement at night. Of note, the results of this study

showed upregulation of specific genes associated with the insulin-like growth factor 2 and ATPase pathway. This has given more evidence and insight into the role the insulin-like growth factor 2 and ATPase pathway may have on underlying the circadian regulation of the electric signal and its energetic cost in *B. gauderio*.

I. Introduction

A. Background

Biological rhythms direct biological processes such as sleep-wake cycles, hormone secretion, and metabolic regulation with respect to certain cyclic time periods (Rana & Mahmood, 2010). Biological clocks are responsible for producing biological rhythms. These biological clocks are endogenous and self-sustained time-keeping systems. The circadian rhythm, a type of biological rhythm, is innate and coordinates living systems to synchronize to the Earth's 24-hour light/dark cycle (Pittendrigh, 1960). The term circadian is derived from the Greek words circa (about) and dian (day) meaning "about a day" (Kulczykowska et al., 2010). The circadian rhythm is seen in practically every organism, ranging from prokaryotes such as cyanobacteria, to plants, insects, and humans (Kulczykowska et al., 2010). Throughout evolution, organisms have coordinated their behavior and physiology in relation to light/dark cycles for survival and reproductive success.

A true circadian rhythm must adhere to two characteristics: it must persist in the absence of external cues, often referred to as free running, and have the ability to be entrained (Pittendrigh, 1960). The first evidence of how a circadian rhythm free runs came from the experiments by Jean Jacques d'Ortous de Mairan, who observed a Mimosa plant in a constant dark room and documented how the plant still opened and closed its leaves matching approximately a 24 hour cycle (Huang, 2018). Biological clocks regulating the circadian rhythm can be entrained by periodic external cues, referred to as zeitgebers. The main zeitgeber that synchronizes the circadian rhythm is light, but there are other cues that can entrain the circadian rhythm, such as social interactions, temperature, and eating behaviors (Quante et al., 2019).

The ability of the circadian rhythm to free run and be entrained is determined by the endogenous molecular machinery of the biological clocks. The molecular components of the biological clocks associated with the circadian rhythm are similar across vertebrates. Genes and proteins vary between different organisms but essentially use the same basic clock mechanism (Figure 1). This mechanism is a molecular transcription-translation feedback loop that follows a 24-hour period (Foster & Kreitzman, 2014). The molecular feedback loop involves positive and negative feedback (Figure 1). The positive loop involves two transcription factors, the circadian locomotor output cycle kaput (CLOCK) and brain and muscle aren't-like 1 (BMAL1) binding to the promoter region of the *period (per)* gene and (*cry*) gene in the early morning (Figure 1). The CLOCK-BMAL1 dimer initiates the transcription of *period* and *cry.* The *per* and *cry* mRNA is then translated into the PER and CRY proteins. Once these proteins begin to accumulate in the cytoplasm, they interact with each other forming CRY-PER dimers (Bass & Takahashi, 2010). The negative portion of the loop occurs during the night. The CRY-PER dimers translocate into the nucleus to interact with the BMAL1-CLOCK dimer to shut off their own transcription (Figure 1). Once the transcription is turned off, the remaining proteins are broken down. The cycle starts all over again in the morning with BMAL1-CLOCK dimer binding to the promoter region.

Circadian rhythms are typically organized in a hierarchical manner. For instance, the mammalian circadian rhythm is controlled by a master clock located in the brain, which drives several peripheral clocks in different tissues (Ko & Takahashi, 2006). The master clock more specifically resides in the suprachiasmatic nucleus (SCN) of the hypothalamus (Bass & Takahashi, 2010). The clock genes and their underlying mechanism are similar in both the brain and peripheral tissues (Ko & Takahashi, 2006). In the SCN, the master clock regulates outputs

including behavioural rhythms, such as sleep-wake cycles and feeding (Bass & Takahashi, 2010). In the peripheral tissues, clocks regulate metabolic rhythms, such as regulation of glucose concentration in blood during fed and fasted states (Bass & Takahashi, 2010).

Circadian clocks regulate metabolic functions. A key peripheral tissue involved in responding to metabolic status is the pancreas. In mice, it has been shown that pancreatic cells have circadian genes (Marcheva et al., 2010). Disruption of the two transcription factors, CLOCK and BMAL1, results in delayed growth, reduced glucose metabolism, and decreased insulin signaling of the pancreatic islets. Peripheral clocks coordinate metabolic responses in relation to light-dark cycles that are specific to the peripheral tissues they reside in. For example, the pancreas secretes insulin during the day time and glucagon in the night time (Bass & Takahashi, 2010). Another example supporting the evidence for the connection between clocks regulating metabolism is the role of the previously mentioned protein CRY, which has been shown to repress gluconeogenesis (Bass & Takahashi, 2010). When looking at energetically expensive tissues such as skeletal muscle, there is strong evidence linking circadian-regulated genes to skeletal muscle physiology (Chatterjee & Ma, 2016). For instance, a significant portion (17%) of genes in skeletal muscles exhibit circadian-like oscillations and nearly 30% of CLOCK-differentially regulated transcripts are involved in metabolism (Chatterjee & Ma, 2016). Based on the information above, circadian clocks play a key role in metabolism and energy production

The timely investment of energy resources is key for survival and reproductive success. This is particularly evident in semelparous species where reproduction is limited to a short window of time. The case study of the frog *Crinina signifera* provides an example of how sexual selection overrules natural selective pressure (Lemckert & Shine, 1993). *C. signifera*'s

reproductive strategy includes high reproductive expenditures that result in an increased risk of mortality. During the breeding season, male *C. signifera* enhance their calling rate and volume to attract mates in the nighttime, allocating a large portion (40%) of their energy budget to this behaviour. Enhanced calling increases the risk of predation and energetic cost within the male *C. signifera*. For instance, in one reproductive season (1987-1988), 73% of male *C. signifera* died, compared to only 57% mortality in females (Lemckert & Shine, 1993). In male *C. signifera* the increased allocation of energy towards their calling behaviour has characterized a trade-off between reproductive success and survival.

The nocturnal gymnotiform fish *Brachyhypopomus gauderio* has emerged as a good candidate model system to study the cellular and molecular mechanisms underlying the circadian regulation of energy metabolism. *B gauderio* produce an electric signal to navigate their environment and communicate with members of their social group. The electric signal (1-2 mV) is referred to as an electric organ discharge (EOD), and it is produced by a specialized bilateral structure known as the electric organ (EO). The EO extends from the fish's operculum to the end of the caudal filament (Bennett, 1971). The EO is composed of an array of box-like individual cells, known as electrocytes. In *B. gauderio*, the electrocytes develop from skeletal muscle, by repressing the expression of the contractile proteins myosin and actin while retaining the ability to produce action potentials (APs) via a nicotinic cholinergic synapse from spinal electromotor neurons (Zakon & Unguez, 1999). The EOD of *B. gauderio* is a biphasic, pulse-type waveform that results from two APs produced in sequence from the two electrogenic membranes of the electrocytes (Figure 2) (Stoddard et al., 1998). Each AP is generated due to the transport of sodium ions into the electrocytes through voltage-gated sodium channels. The first phase of the EOD waveform, P1, is generated when sodium ions enter the posterior membrane of the

electrocyte through voltage-gated sodium channels, while the second phase, P2, is generated when sodium ions enter the anterior membrane of the electrocyte through voltage-gated sodium channels (Figure 2) (Stoddard et al., 1998). Stoddard and Markham (2018) showed that both membranes depolarize simultaneously, but P1 rises ahead of P2 which can be attributed to the positive phase (Figure 2). As such, P1 begins to repolarize by the influx of K^+ while P2 is still depolarizing which results in the negative phase (Stoddard & Markham, 2008; Figure 2). The sum of the APs on across a single electrocyte's posterior and anterior membranes is known as the microEOD (μEOD).

The EOD in *B. gauderio* follows a circadian rhythm that differs between sexes. Over time, male *B. gauderio* have evolved the ability to attract females at night while conserving energy in the daytime, leading to the evolution of cellular and genetic mechanisms to alter EOD parameters at different times of the day (Hopkins, 1999). *B. gauderio* display day-night oscillations in their EOD's amplitude, duration, and discharge rates (Figure 3) (Stoddard et al., 2007). Even though day-night oscillation is seen in both sexes, they are more pronounced in male *B. gauderio* (Stoddard et al., 2007; Figure 3). Reproductively active males generate EODs with larger amplitude and longer duration, and further enhance their EODs in the nighttime during the hours of spawning and courtship (Franchina & Stoddard, 1998; Silva et al., 1999). The enhancement in the male EOD can be attributed to mate attraction and competition. Female *B. gauderio* are more likely to choose larger males (Curtis & Stoddard, 2003), and male body size positively correlates with the amplitude and duration of their EOD (Franchina & Stoddard, 1998). Males use their EODs to communicate their body condition to potential mates other competing males (Franchina & Stoddard, 1998). The exaggerated amplitude and duration of the EOD in males is positively correlated with reproductive success (Salazar & Stoddard, 2008).

Male *B. gauderio*'s EOD circadian rhythm poses a unique opportunity to study how the trade-off between survival and reproduction has been partially resolved by regulating the investment of energy allocation to reproductive behaviors. Nighttime EOD enhancement in male *B. gauderio* gives a reproductive advantage at the expense of increased predation risk and energetic costs. The EOD can be detected by electroreceptive predators, such as the catfish *Rhamdia quelen*. Thus, enhancement of EOD poses a greater predation risk to *B. gauderio* (Dunlap et al., 2017; Gavassa et al., 2017). A huge portion of *B. gauderio* males' energy budget (between 11-22%) is spent on signal generation, compared to females with only 3% allocated to signal generation (Salazar & Stoddard, 2008). Similarly to the previously mentioned frog *C. signifera*, *B. gauderio* is a semelparous species where males display a trade-off between energy allocated to signalling, self-maintenance, and survival to achieve reproductive success (Stoddard & Salazar, 2011). For instance, in male *B. gauderio*, there is an inverse correlation with energy spent on metabolism and energy spent on electric signalling, whereas in females, these two aspects are positively correlated (Stoddard & Salazar, 2011; Figure 4).

The circadian rhythmicity of the EOD enhancement seen in male *B. gauderio* can be mimicked pharmacologically through injection of specific hormones, such as the melanocortins adrenocorticotropic hormone (ACTH) and alpha melanocyte stimulating hormone (α-MSH) (Markham et al., 2009; Markham & Stoddard, 2005). The hypothalamic-pituitary-adrenal axis regulates the release in circulation of ACTH and α-MSH, which enhance the EOD (Markham, Allee, et al., 2009). The EOD enhancement is mediated by the cyclic AMP signaling mechanism (Markham & Stoddard, 2005). The cyclic AMP signaling mechanism is initiated when ACTH binds to the cell membrane receptor melanocortin receptor 5 (MC5R), a G-protein coupled

receptor which activates a G protein (Sassone-Corsi, 2012). The activated G protein in turn activates the enzyme adenylyl cyclase, which then converts ATP to cAMP. The second messenger cAMP then activates protein kinase that is responsible for the phosphorylation of certain proteins to initiate alteration in cellular activity. Lee (2018) was able to isolate and characterize a complete MC5R gene in both male and female *B.gauderio* on day-night cycles that is likely the receptor mediating the melanocortin-driven EOD plasticity. Intramuscular injections of ACTH increase EOD amplitude and duration within minutes and ACTH applied directly to electrocytes increases the μEOD (Markham & Stoddard, 2005). The enhancement of the μEOD results from an increasing interval between the two APs of the electrocytes.

Proceeding an AP, membrane bound proteins known as Na^+/K^+ ATPases restore the resting membrane potential (RMP) of the electrocytes (Lewis et al., 2014). For every ATP hydrolyzed by this ATPases, 3 sodium ions are exported and 2 potassium ions are imported to the electrocyte (Figure 5). These ATPase proteins are energetically costly. Energetic studies in a close relative of *B. gauderio*, the gymnotiform species *Eigenmannia virescens*, have shown that each electrocyte requires approximately $2.1 \pm 0.2 \times 10^{10}$ ATP molecules per EOD to reset the RMP (Lewis et al., 2014). Given that the EOD has a higher frequency and amplitude at night, the Na^+/K^+ ATPases need to reset the RMP at a faster rate and thus there is increased metabolic demand in the electrocyte.

B. Gap of Knowledge and Proposed Research

As previously stated, *B. gauderio* exhibit a circadian regulated EOD. The enhancement in amplitude and duration in the males at night is attributed to reproductive success by mate attraction and repelling competitors. However, this masculinity nighttime EOD also incurs costs,

mainly an increase in predation detection and higher energetic expense. The work conducted by Michael Markham and colleagues in 2005 and 2009 demonstrated that melanocortins such as ACTH mimic the same effect the night cycle has on the EOD. His work gave insight to the role the cAMP signaling mechanism has on EOD regulation.

In addition, previous work on energetically expensive tissue like skeletal muscle has shown how biological clocks can regulate metabolic functions. Since the electric organ in *B. gauderio* is derived from skeletal muscle, this allows for studying the molecular mechanism that connects the circadian rhythm to energy regulation in the electric fish. Energy balance is one of the most important key factors of metabolic processes and we have the unique opportunity to see how this connection supports important aspects of reproductive behaviours.

For my Honours thesis, I investigated the differential circadian gene expression in the electric organ of male and female *B. gauderio*. I predict that genes associated with the EO's clock machinery, melanocortin signaling pathways, and metabolic function will be upregulated in the nighttime fish. I also predict the genes associated with EOD production, such as the voltage gated sodium ion channels, voltage gated potassium channels, and the sodium/potassium ATPases, will be upregulated in nighttime fish.

II. Materials and Methods

A. Animal Care and Housing Conditions

The Behavioural Neuroendocrinology lab at Cape Breton University (CBU) houses a colony of the gymnotiform fish, *B. gauderio.* The subjects of this experiment were sexually mature *B. gauderio*. Fish were be kept in aquaria filled with filtered water treated with Stress Coat® (API), Cycle (Nutrafin) and Walter's solution. These water conditioners maintained a

balance of beneficial bacteria and electrolytes in the tanks' water. The water was kept at a conductivity of 70-100µS/cm, pH at 6.5-7.0 and temperature at 25-30°C. These ranges mimic *B. gauderio's* environmental conditions during its natural breeding season (Silva et al., 2003; Giora et al., 2014; Crampton et al., 2016). *B. gauderio* were kept on a 12:12 dark-light cycle to maintain the circadian rhythm and breeding behaviour. Two groups of fish were separated into two rooms; Room 1 experienced the light cycle between 4:30AM-4:30PM and Room 2 experienced the light cycle between 8:00PM-8:00AM. These times were chosen to facilitate practical collection of samples during the daytime hours at 10:30AM. Each room consisted of two experimental tanks containing a male and female pair. Fish were fed daily a mixed diet of frozen bloodworms, brine shrimp, *Daphnia*, and live black worms. All animal care and use protocols followed the standards of the Canadian Council on Animal Care and were approved by the CBU Animal Care Committee (AUP# 1516-003).

B. Overview of Experimental Design for Quantification of Gene Expression

A sample size of 8 fish was used across four experimental groups: 2 day females, 2 day males, 2 night females, and 2 night males. Tail segments measuring 1-cm were sampled from both night and day fish. The daytime fish were sampled halfway through the light cycle at 10:30AM; this is demonstrated to be the time when the EOD on average is at its minimum amplitude and duration (Franchina & Stoddard, 1998). The nighttime fish were sampled 2.5-hours after the onset of dark cycle; this has been demonstrated to be the time when the EOD on average is at its maximum amplitude and duration (Franchina & Stoddard, 1998). The skin was carefully removed from the tail segments under a dissecting microscope (Olympus, BH-2 compound microscope). RNA extraction was performed on the tail segments and then tested for

quantity, purity, and fragmentation. Direct RNA sequencing was conducted using RNA samples from the four experimental groups. A bioinformatics analyses pipeline (see Data Analysis section) was then used to identify and quantify differences in gene expression between day and night in males and females *B. gauderio* (Figure 6).

C. Signal Recording

Sample fish were placed in a recording tub filled with reverse osmosis water treated with Stress Coat® (API), Cycle (Nutrafin) and Walter's solution. The recording tank consists of a tube-like structure made out of mesh fabric, positioned in the center of the tank, and three electrodes: one ground, one positive, and one negative. The electrodes were connected to an oscilloscope which was used to visualize the EOD.

D. Tissue Sampling

Once the signal was recorded the fish was taken out of the experimental tank and a 1-cm segment from the most caudal region of the tail was cut. This region of the tail contains a high amount of electrocytes and has high regenerative capacity. In the wild, many fish experience damage to their tails due to predation attempts and are able to regenerate the lost tissue (Hopkins, 1991). To limit any stress that is mediated by the tail clipping, the process was limited to approximately 3 minutes. Stress Coat® was then applied to the wound and the fish was immediately placed back in its original tank and monitored over the next few days. The cut tail segment was placed in RNAlater® (Applied BioSystems) until the dissection took place to reduce degradation of the RNA sample.

E. Electrocyte Dissection and RNA Extraction

Each 1-cm tail segment was placed under a dissection microscope to carefully remove the skin and expose the electrocytes. The dissection was limited to approximately 80 minutes to reduce RNA degradation; however, some took longer than others. The skinless tail segment was placed in 1ml of RNAlater® and stored in the 4°C fridge until RNA extraction. RNA was extracted using the Direct-zol RNA MiniPrep Kit (Zymo Research) and RNAse away was use continuously throughout this process to reduce the risk of RNA degradation. Once RNA was extracted, the sample was stored in the -20°C freezer. To assess the quantity and purity of each RNA sample, 1µl of each sample was measured in a NanoDrop 8000 Spectrophotometer (ThermoScientific). RNA samples with absorbance ratios of A260/A230 between 2.0 - 2.2 and A260/A280 between 1.8- 2.0 are considered pure and were used for further applications. The fragmentation of the RNA was tested using the Qubit™ 4 Fluorometer (Invitrogen). If RNA is fragmented it can affect the read length distribution from the direct RNA sequencing (Prawer et al., 2023). It is preferable to use RNA samples with a RNA Quality Indicator (RQI) value ≥ 6.6 in direct RNA sequencing using the Oxford Nanopore sequencing, because this sequencing approach benefits from having large RNA fragments (Taylor *et al*., 2010). However, it has been shown in other published work that highly fragmented RNA samples can still be sequenced with good stability, but may require additional computational power and time for the analysis pipeline (Li et al., 2024).

F. Direct RNA Sequencing

Direct RNA sequencing was performed using the Oxford Nanopore MinION sequencer (Oxford Nanopore Technologies). There are three steps involved in this process: library

preparation, sequencing run, and basecalling. Library preparation took ~115 minutes and involved synthesizing the DNA complementary strand (cDNA) using the enzyme SuperScript III reverse transcriptase (Invitrogen) to stabilize the RNA. The library preparation step also involved adding sequence adapters to enable the RNA to be pulled through the pores of the flow cell. A flongle flow cell was tested to ensure it had an adequate number of pores. Flow cells that had between 70-80 pores were used. Once the library preparation step was completed, the flow cell was primed and loaded with 30µl of the prepared RNA, and then the sequencing run was launched. The sequencing run used the MinKNOW software on a high-performance laptop (ASUS) and was left to run for 24 hours. The raw sequenced data from the MinKNOW was then basecalled into RNA reads by the basecaller Guppy application.

G. Data Analyses

The pipeline that I used to analyze my sequencing data followed these major steps: alignment of reads to the reference transcriptome using Minimap2, quantification of transcripts using Nanocount, and finally determining the differential expression of transcripts using DESeq2. Upon completion of basecalling, the sequencing reads were checked for length and quality. Sequencing reads with a quality score equal or higher than 7 were used for downstream analyses. The assembler Canu was used to trim and assemble the reads into corrected consensus sequences. Using the Minimap2 application, each sequence was mapped to the reference annotated transcriptome for *B. gauderio* (curated in the Michigan State University repository by Dr. Jason Gallant at http://efishgenomics.com) to identify unique transcripts in each EO sample. Quantification of transcripts was performed using the Nanocount application. The transcriptome generated for each EO sample was accompanied by its own unique annotation to be fed into the

next step of the pipeline. Differential expression of transcripts across samples was determined using the statistical tool DESeq2, executed as an embedded package with the statistical R platform.

III. Results

A. Sampled fish displayed previously documented EOD circadian pattern

As shown in previous studies, both males and females enhance their EOD amplitude and duration in the nighttime compared to daytime values (Franchina and Stoddard, 1998) (Table C). Also consistent with data from previous studies, the day-to-night change in the EOD amplitude and duration observed in my sampled males was larger than the change observed in my sampled females (Table C). My recorded EODs fell within the expected range for the daytime low and nighttime high when comparing them to those reported by Franchina and Stoddard (1998). Thus, confirming that I am capturing the expected EOD circadian cyclicity as well as the extreme ends of this cycle for both male and female *B. gauderio.*

B. Assessment of RNA quantity, purity, and fragmentation

An essential step in my protocol required ensuring that the quantity and quality of my RNA samples were sufficient to proceed into the sequencing protocol. For my male samples, my RNA concentrations ranged from 141.90 ng/µL to 217.60 ng/µL and for my female samples, my RNA concentrations range from 86.20 ng/µL to 158.00 ng/µL (Table A). These RNA concentrations were sufficient to carry my samples through the sequencing protocol.

To assess the purity of my RNA samples, I measured the absorbance of each sample at three wavelengths: 230, 260, and 280 nm. These absorbance values were used to calculate the

260/230 and 260/280 ratios (Table A). These ratios allowed me to estimate the level of contamination from proteins and the RNA extraction kit's reagents, respectively. All of my RNA samples were within the range of purity for these calculated ratios (Table A).

I also measured the level of fragmentation (i.e., nucleotide length of the RNA mixture in each sample) in my RNA samples to estimate whether my samples had more small or large fragments. Two of my female RNA samples had a concentration that was lower than was needed to calculate the fragmentation value using the Qubit RNA IQ Assay (Table B). The rest of my RNA samples displayed scores that indicated a higher representation of smaller fragments relative to larger samples (Table B). Having a larger number of smaller fragments in my sample meant that mapping of my reads to the reference transcriptome, as part of the differential expression analysis pipeline, was going to be more computationally challenging and time-consuming. Another limitation could be that I wasn't able to capture all the genes. If the software was having difficulty trying to map small fragments it could skip over that region.

C. Assessment of read length distribution and read quality for RNA sequences

After the completion of basecalling, the reads output from each RNA sample sequenced were checked for read length distribution and read quality to ensure adequate values before moving into the analysis pipeline. The read length and read quality was determined using the wf-transcriptomes Netflow workflow (Oxford Nanopore Technologies). Despite having a larger representation of smaller fragments in my RNA samples when looking at the read length distribution, I was able to obtain some large fragments in the kilobase range for males (Figure A) and females (Figure B). For my female samples, the mean read length distribution ranged from 428 to 544 bases (Table 1). For my male RNA samples, the mean read length distribution ranged

from 400 to 698 bases (Table 2a). An additional 4 males (2 daytime and 2 nighttime) were added to the data set to increase the sample size for males. These males were sampled in the Summer of 2023, under the same conditions that I used for my study. For these additional males, the mean read length distribution ranged from 441 to 898 bases (Table 2b).

I also checked the read quality for each RNA sample sequenced. The mean quality score gave me an estimation on the probability of basecalling error within my RNA sequences. In order to prevent inaccurate results at the end of the analysis pipeline I used a read quality cut off of 7. All of my RNA sequences for both male (Tables 2a and 2b) and female (Table 1) samples were above the read quality cut off and carried through the rest of the analysis pipeline.

D. Differential gene expression results

Once the basecalled reads for each male and female sample were mapped to the annotated reference transcriptome, reads could be grouped across their mapped gene regions, generating a list of genes with mapped reads in the transcriptome as well as counts of reads mapped to these gene regions. Only RNA transcripts (corresponding to genes in the reference transcriptome that code for proteins) were included in the rest of the pipeline analysis. In order to accurately compare across replicates of each sample type (e.g., across four male daytime samples), a normalized comparable metric is needed to assess how many reads mapped in one sample versus the other across each coding gene with mapped reads. For each sample, the read counts mapped to each coding gene region in the reference transcriptome were normalized for sequencing depth and gene length. First, to normalize for sequencing depth, counts per million (CPM), the number of mapped reads to a particular gene adjusted to a million scaling factor, were calculated. In addition, to further normalize for gene length, the transcripts per kilobase

million (TPM) were calculated by dividing the read counts by the length of each gene in kilobases, then counting all the reads per kilobase (RPK) in a sample, and finally dividing the RPK values by the per million scaling factor. The highest TPMs obtained from the 8 day-night males were divided into 4 different categories: Metabolic Function, Vesicle Trafficking, Calcium Signaling, and Protein Translation, with the averages of daytime and nighttime TPM summarized in Table 3.

To quantify differentially expressed genes (DEGs) in *B. gauderio* male EOs, between day and night, fold change (FC) was calculated. FC measures the quantity of change between an experimental condition (i.e., nighttime condition) in relation to a control condition (i.e., daytime). As such, FC values provide a metric of gene expression change observed during the night relative to the day. To visualize the differences between nighttime and daytime samples for each sex, MA plots were generated. Accordingly, log2(FC) values (M) were plotted against average log2(CPM) values (A) to determine the distribution of up-down regulated genes across the average normalized counts in males (Figure 7A) and females (Figure 7B). Log2(FC) values >1 corresponds to upregulated genes, while log2(FC) and values < -1 corresponds to down regulated genes (Figure 7).

To further visualize the difference between nighttime samples and daytime samples for each sex, bar graphs were generated. From this analysis, in male *B. gauderio*, I identified 231 upregulated genes and 108 downregulated genes in the nighttime compared to the daytime (Figure 8A). In female *B. gauderio*, I identified 32 upregulated and 36 downregulated genes in the nighttime compared to the daytime (Figure 8B).

To determine which DEGs were statistically significant between nighttime samples and daytime samples for each sex, I used the false discovery rate (FDR) statistical approach. When

looking at the whole transcriptome of the EO which is a high-throughput experiment (high amount of data), FDR was used to correct for random events that falsely appear significant. This approach allowed me to identify as many significant comparisons as possible between nighttime in relation to daytime while still maintaining a low false positive rate. To visualize DEGs that were statistically significant, I generated volcano plots, where -log10(FDR) values were plotted against log2(FC). These plots revealed that a statistically significant portion of genes were up regulated and downregulated in nighttime male *B. gauderio* compared to daytime (Figure 9A). For males, log2(FC) values > +1 and above the 0.1 threshold for –log10(FDR) (purple dots) are DEGs that are significantly upregulated in the nighttime compared to the daytime, while log2(FC) values < -1 and above the 0.1 threshold for –log10(FDR) (orange dots) are DEGs that are downregulated in the nighttime compared to the daytime. Log2(FC) values that are between -1 and 1 and below the 0.1 threshold for –log10(FDR) (grey points) represent no significant DEGs. For female samples, there were few to no DEGs that were significantly upregulated or downregulated in the nighttime compared to the daytime (Figure 9B). Since males had a much larger number of significant DEGs compared to females, further analysis focused on the male samples only.

Of the DEGs that were significant in the nighttime male, I categorized specific genes that code for proteins that have been previously shown to be involved in circadian regulation, energy balance and metabolism, as well as in EOD generation and plasticity in *B. gauderio*. These categories consisted of: Circadian Core Clocks, Clock-Controlled Genes, Metabolic Pathways, Vesicle Trafficking, Insulin & Growth Hormone Signalling, Endocrine Metabolic Regulation, Other Endocrine Regulation, and Electrogenesis (Table 4).

The category circadian core clock genes consist of genes that are upregulated, such as CLOCK *per*, *cry* and ARNTL2 which is the precursor for BMAL1 (Table 4). These genes endogenously generate the circadian rhythm by transcriptional-translational feedback loops. The category clock controlled genes consists of genes that are upregulated and controlled by the core clock genes. These mostly include transcription factors involved in metabolism (Table 4). The category metabolic pathway consists of genes that are upregulated and associated with metabolic regulation such as creatine phosphate as well as genes involved in the electron chain transport (Table 4). Furthermore, the category vesicle trafficking consists of genes that are upregulated and associated with moving proteins into the electrocyte membrane (Table 4). The category insulin & growth hormone signalling pathway consists of genes that are upregulated and part of the insulin like growth factor 2 and ATPase pathway (Table 4). The endocrine metabolic regulation category consists of the leptin receptor that I found to be downregulated in the nighttime male *B. gauderio* (Table 4). The endocrine regulation other category consists of the upregulation of MC5R and androgen receptor in the EO of male *B. gauderio* (Table 4). Finally, the electrogenesis category consists of the upregulation of genes that are responsible for producing the EOD, such as, *scn4aa* and *atp1a2a* (Table 4). Some categories consist of the same gene listed more than once. This can be attributed to more than one transcript aligning to that specific gene region of the reference transcriptome.

IV. Discussion

The main objective of this Honours thesis project was to determine the differential circadian gene expression in the electric organ of male and female *B. gauderio.* The results of this study have confirmed the upregulation of certain genes associated with metabolic pathways

that have been shown in previous work to mediate EOD plasticity, as well as the important role circadian clocks have on metabolic regulation in order to support the EOD enhancement. Furthermore, my project has provided more evidence to support the hypothesis that the insulin-like growth factor 2 and ATPase pathway is an important molecular mechanism underlying the circadian regulation of the EOD and its energetic costs.

A. Sex differences in gene differential expression

The number of genes that were upregulated and down regulated during the nighttime relative to the daytime varied between sexes. When looking at the MA plots, males displayed a higher number of both upregulated and downregulated genes compared to females (Figures 8 and 9). This trend was even more pronounced when looking at the volcano plots for the number of DEGs that were significant. Females had a fewer number of significant DEGs compared to males (Figure 9). This could be attributed to two reasons: i) the sample size (including number of fish sampled as well as number of reads obtained per sample) and ii) the documented circadian rhythm differences between male and female *B. gauderio*. The sample size in females (n=4) was smaller compared to males' sample size (n=8). As well, the reads in female samples (Figure B) compared to male samples (Figure A) were fewer.

The difference in circadian regulation of the EOD between *B. gauderio* sexes could also be a reason why I found less DEGs. Both sexes increase their amplitude and duration in nighttime compared to daytime. However, even though day-night oscillations are seen in females, they show very little to no change in their nighttime EOD compared to males (Stoddard et al., 2007; Figure 3). It is important to remember that male *B. gauderio* have evolved the ability to enhance their EOD at night to attract females and repel competitors, while reducing their EOD

during the day to conserve energy (Hopkins, 1999). The exaggerated amplitude and duration of the EOD in males is positively correlated with reproductive success (Salazar & Stoddard, 2008). As stated before, males allocate around 22% of their energy budget towards signal production whereas females only allocate around 3% (Salazar & Stoddard, 2008). Since females do not allocate a larger portion of their energy budget or enhance their EOD during the nightime near as much as males, this could explain the lack of significant DEGs as well as the small amount up-down regulated genes.

B. Interpretation of DEGs in the context of previously described mechanisms regulating EOD plasticity

Previous work has identified different mechanisms associated with the EOD nighttime enhancement. I was able to confirm the upregulation of genes that are associated with those mechanisms. Androgens, for example, are thought to modulate EOD plasticity especially during breeding season (Silva et al., 2002). In other weakly electric fish belonging to the genus *Sternopygus* androgens increase the EOD duration (Few & Zakon, 2001). Stacey Lee (2018), as part of her Honours thesis research, characterized the androgen receptor in our fish, *B. gauderio* and my study confirmed the upregulation of androgen receptors in the EO of male *B. gauderio*, further implicating their contribution to the male EOD increase seen in the nightttime fish.

Melanocortins are also a key modulator of EOD plasticity (Markham, Allee, et al., 2009; Markham & Stoddard, 2005). Markham and his colleagues demonstrated that melanocortins, such as ACTH, mimic the same effect the night cycle has on the EOD. ACTH is believed to modulate the EOD by the cAMP pathway. Blocking certain elements of the cAMP pathway, such as protein kinase A (PKA), inhibit ACTH from eliciting the normal enhanced EOD

response (Markham & Stoddard, 2005). As well, the treatment of electrocytes with a cAMP derivative generated an EOD response similar to what is seen when treated with ACTH (Markham et al., 2009). Their work gave insight into the role the cAMP signalling mechanism has on EOD regulation. Stacey Lee (2018) was able to characterize the MC5R in the EO of *B. gauderio* providing evidence that this receptor is likely responsible for mediating the melanocortin-driven EOD plasticity. I was able to confirm the upregulation of MC5R in the nighttime males compared to the daytime (Table 4), giving further evidence that melanocortins via the MC5R and its associated cAMP pathway are likely an important mechanism mediating the EOD nighttime enhancement in *B. gauderio*.

The melanocortin pathway has also been linked to vesicle trafficking of sodium channels to allow for EOD plasticity (Markham et al., 2009). In *Sternopygus macrurus*, the binding of ACTH activates the cAMP, cAMP then actives PKA which induces exocytosis of sodium channels into the electrocyte membrane. More sodium channels in the membrane allows for an increase influx of sodium, thus enhancing the EOD. One gene in particular that is associated with the enhanced EOD is *scn4aa*. This gene codes for the voltage-gated sodium channel SCN4Aa, a membrane protein that allows for transport of sodium ions into the electrocyte during the onset of an AP, depolarizing the electrocyte and generating an EOD (Zakon et al., 2006). Gallant and colleagues' work showed that *scn4aa* was upregulated in the EO of all electric fish species that were in their study (Gallant et al., 2014). Victoria Ivey (2019), as part of her Honours thesis research, was able to confirm the expression of *scn4aa* in the EO of *B. gauderio*. My study has shown that *scn4aa* expression is upregulated in the EO of nighttime *B. gauderio* males as well as genes that are associated with vesicle trafficking (Table 4). My results have given evidence that *B. gauderio* show similar mechanisms behind enhancing their EOD as *S. macrurus*.

C. The upregulation of core clock genes that play a role in metabolism

Circadian rhythms are important in regulating many different biological processes, an important one being metabolic regulation. In *B. gauderio* the regulation of metabolism plays a key factor in EOD plasticity. It is important to remember that electrocytes, the cells responsible for producing EODs, are derived from skeletal muscle. As previously mentioned, skeletal muscle is a highly energetic tissue that has been shown to have ~17% of genes that exhibit circadian-like oscillations and nearly 30% of CLOCK-differentially regulated transcripts are involved in metabolism in other species (Chatterjee & Ma, 2016). Since EODs display circadian regulation, core clock genes are important for allowing metabolic regulation for the increased EOD seen at nighttime especially in male *B. gauderio*. My study confirmed the upregulation of CLOCK, BMAL1, PER 1 and other core clock proteins (Table 4). Along with the core clock genes, I was able to find the upregulation of clock-controlled genes (CCGs) (Table 4). Most of these CCGs code for transcription factors that are involved in regulating metabolism such as nuclear receptors (Francis et al., 2003).

The importance of circadian clocks has been further supported by a study conducted in skeletal muscle in mice (Malhan et al., 2023). This study determined that circadian functioning is crucial to maintaining physiological alterations and musculoskeletal atrophy in the mice (Malhan et al., 2023). This study by Malhan and colleagues, along with the upregulation of core clock genes and CCGs that I identified in nighttime male *B. gauderio,* provides more evidence to the key role circadian clocks play in metabolism and energy production.

D. Insulin-like growth factor 2 and ATPase pathway as a mediator of metabolic regulation and EOD plasticity

The insulin-like growth factor 2 and ATPase pathway has emerged as a promising mediator of EOD plasticity as well as dealing with the energetic cost of EOD production. The work of Gallant and colleagues has suggested a cellular pathway linking the metabolic action of IGF-II and the trafficking of Na^+/K^+ ATPases (Gallant et al., 2014; Figure 10). The pathway suggests that the binding of IGF-II to the IGF receptor (IGFR) activates the insulin receptor substrate 1 protein (IRS1), which in turn activates phosphoinositide 3 kinase (PI3K), phosphorylating zinc and ring finger protein 2a (ZNRF2a) which directly traffics Na^+/K^+ ATPases into the electrocyte membrane (Gallant *et al*., 2014). Ivey (2019) was able to confirm the expression *of igf2* and *atp1a2a* in the EO of *B. gauderio*. I was able to identify the upregulation of *igf2*, *igfr*, *irs2, pI3K* and *atp1a2a* highlighted in red boxes seen in Figure 10.

The binding of IGF-II in the EO has an end result of trafficking more Na^+/K^+ ATPases into the cell membrane (Figure 11). During the nighttime, male *B. gauderio* enhance the size of their EOD and the frequency of EOD production. As such, the resting membrane potential of the electrocytes needs to be reset at a quicker rate to allow for more APs to be produced. Trafficking more Na^+/K^+ ATPases into the cell membrane of electrocytes will increase their repolarization capabilities to support the production of EODs at a faster rate.

This pathway not only results in the trafficking of Na^+/K^+ ATPases into the membrane but also glucose transporter 4 (GLUT4). Since electrocytes are derived from skeletal muscle they package GLUT4 in cytoplasmic vesicles, once insulin binds these GLUT4 are translocated into the cell membrane to allow for the uptake of glucose (Wang et al., 2020). Since IGF-II has similar sequence, structure, and biological functions as insulin it plays a metabolic role in

glucose transport and utilization (O'Dell & Day, 1998). When IGF-II binds its receptor, the activation of pI3K can lead to the trafficking of Na^+/K^+ ATPases into the membrane but also trafficking GLUT4 into the membrane. This allows for an increase in energy production to sustain the metabolic demands of the enhanced EOD (Figure 11).

V. Conclusions and future directions

In conclusion, in male *B. gauderio*, I have successfully identified 231 genes that were upregulated, and 108 genes that were downregulated in the electric organ at nighttime. Of those genes, I have also identified genes that were significantly differentially expressed and play a critical role in the fish's biology. An important and exciting result of my project is that the insulin-like growth factor 2 pathway likely plays a role in supporting the metabolic needs of the electric organ, facilitating the nighttime EOD increase in male *B. gauderio.* Further work would include characterizing the components of this pathway as well as performing pharmacological and behavioral studies by injecting antagonists to certain elements in the insulin-like growth factor 2 and ATPase pathway and recording the EODs to measure any deficits on the nighttime increase.

References

Bass, J., & Takahashi, J. S. (2010). Circadian integration of metabolism and energetics. *Science (New York, N.Y.)*, *330*(6009), 1349–1354. https://doi.org/10.1126/science.1195027

Bennett, M. V. L. (1971). Electric Organs. In W. S. Hoar & D. J. Randall (Eds.), *Fish Physiology* (Vol. 5, pp. 347–491). Academic Press. https://doi.org/10.1016/S1546-5098(08)60051-5

Chatterjee, S., & Ma, K. (2016). Circadian clock regulation of skeletal muscle growth and repair. *F1000Research*, *5*, 1549. https://doi.org/10.12688/f1000research.9076.1

Curtis, C. C., & Stoddard, P. K. (2003). Mate preference in female electric fish, *Brachyhypopomus pinnicaudatus*. *Animal Behaviour*, *66*(2), 329–336. https://doi.org/10.1006/anbe.2003.2216

Few, W. P., & Zakon, H. H. (2001). Androgens alter electric organ discharge pulse duration despite stability in electric organ discharge frequency. *Hormones and Behavior*, *40*(3), 434–442. https://doi.org/10.1006/hbeh.2001.1709

Foster, R. G., & Kreitzman, L. (2014). The rhythms of life: What your body clock means to you! *Experimental Physiology*, *99*(4), 599–606. https://doi.org/10.1113/expphysiol.2012.071118

Franchina, C. R., Salazar, V. L., Volmar, C.-H., & Stoddard, P. K. (2001). Plasticity of the electric organ discharge waveform of male *Brachyhypopomus pinnicaudatus*. II. Social effects. *Journal of Comparative Physiology A: Sensory, Neural, and Behavioral Physiology*, *187*(1), 45–52. https://doi.org/10.1007/s003590000176

Franchina, C. R., & Stoddard, P. K. (1998). Plasticity of the electric organ discharge waveform of the electric fish *Brachyhypopomus pinnicaudatus* I. Quantification of day-night

changes. *Journal of Comparative Physiology A: Sensory, Neural, and Behavioral Physiology*, *183*(6), 759–768. https://doi.org/10.1007/s003590050299

Francis, G. A., Fayard, E., Picard, F., & Auwerx, J. (2003). Nuclear Receptors and the Control of Metabolism: Annual Review of Physiology. *Annual Review of Physiology*, *65*(1), 261. https://doi.org/10.1146/annurev.physiol.65.092101.142528

Gallant, J. R., Traeger, L. L., Volkening, J. D., Moffett, H., Chen, P.-H., Novina, C. D., Phillips, G. N., Anand, R., Wells, G. B., Pinch, M., Güth, R., Unguez, G. A., Albert, J. S., Zakon, H. H., Samanta, M. P., & Sussman, M. R. (2014). Genomic basis for the convergent evolution of electric organs. *Science (New York, N.Y.)*, *344*(6191), 1522–1525. https://doi.org/10.1126/science.1254432

Hall, J. C., Rosbash, M., & Young, M. W. (n.d.). *The 2017 Nobel Prize in Physiology or Medicine*.

Herzog, E. D. (2007). Neurons and networks in daily rhythms. *Nature Reviews Neuroscience*, *8*(10), 790–802. https://doi.org/10.1038/nrn2215

Hopkins, C. D. (1991). *Hypopomus pinnicaudatus* (Hypopomidae), a New Species of Gymnotiform Fish from French Guiana. *Copeia*, *1991*(1), 151–161. https://doi.org/10.2307/1446259

Hopkins, C. D. (1999). Design features for electric communication. *Journal of Experimental Biology*, *202*(10), 1217–1228. https://doi.org/10.1242/jeb.202.10.1217

Ivey, V. (2019). Characterization of IGF-IIA and IGF-IIB proteins and differential temporal and sex-linked expression of igf2b, atp1a2a, and scn4aa genes in the electric organ of the Gymnotiform fish *Brachyhypopomus gauderio* (Unpublished Honors Thesis). Cape Breton University, Sydney, NS, Canada.

Ko, C. H., & Takahashi, J. S. (2006). Molecular components of the mammalian circadian clock. *Human Molecular Genetics*, *15*(suppl_2), R271–R277. https://doi.org/10.1093/hmg/ddl207

Kulczykowska, E., Popek, W., & Kapoor, B. G. (2010). Biological Clock in Fish. *Chemical Rubber Co Press,* 1-7.

Lemckert, F. L., & Shine, R. (1993). Costs of Reproduction in a Population of the Frog *Crinia signifera* (Anura: Myobatrachidae) from Southeastern Australia. *Journal of Herpetology*, *27*(4), 420–425. https://doi.org/10.2307/1564830

Lewis, J. E., Gilmour, K. M., Moorhead, M. J., Perry, S. F., & Markham, M. R. (2014). Action potential energetics at the organismal level reveal a trade-off in efficiency at high firing rates. *The Journal of Neuroscience: The Official Journal of the Society for Neuroscience*, *34*(1), 197–201. https://doi.org/10.1523/JNEUROSCI.3180-13.2014

Lee, S. (2018). Circadian and sex-linked gene expression of melanocortin receptor 5 and androgen receptor in the electric organ of *Brachyhypopomus gauderio* (Unpublished Honors Thesis). Cape Breton University, Sydney, NS, Canada.

Li, S., Liu, J., Zhao, M., Su, Y., Cong, B., & Wang, Z. (2024). RNA quality score evaluation: A preliminary study of RNA integrity number (RIN) and RNA integrity and quality number (RNA IQ). *Forensic Science International*, *357*, 111976. https://doi.org/10.1016/j.forsciint.2024.111976

Malhan, D., Yalçin, M., Schoenrock, B., Blottner, D., & Relógio, A. (2023). Skeletal muscle gene expression dysregulation in long-term spaceflights and aging is clock-dependent. *Nature Project Journal Microgravity*, *9*(1), 1–20. https://doi.org/10.1038/s41526-023-00273-4

Marcheva, B., Ramsey, K. M., Buhr, E. D., Kobayashi, Y., Su, H., Ko, C. H., Ivanova, G., Omura, C., Mo, S., Vitaterna, M. H., Lopez, J. P., Philipson, L. H., Bradfield, C. A., Crosby, S. D., JeBailey, L., Wang, X., Takahashi, J. S., & Bass, J. (2010). Disruption of the clock components CLOCK and BMAL1 leads to hypoinsulinaemia and diabetes. *Nature*, *466*(7306), Article 7306. https://doi.org/10.1038/nature09253

Markham, M. R., Allee, S. J., Goldina, A., & Stoddard, P. K. (2009). Melanocortins regulate the electric waveforms of gymnotiform electric fish. *Hormones and Behavior*, *55*(2), 306–313. https://doi.org/10.1016/j.yhbeh.2008.11.002

Markham, M. R., McAnelly, M. L., Stoddard, P. K., & Zakon, H. H. (2009). Circadian and Social Cues Regulate Ion Channel Trafficking. *Public Library of Science Biology*, *7*(9), e1000203. https://doi.org/10.1371/journal.pbio.1000203

Markham, M. R., & Stoddard, P. K. (2005). Adrenocorticotropic Hormone Enhances the Masculinity of an Electric Communication Signal by Modulating the Waveform and Timing of Action Potentials within Individual Cells. *The Journal of Neuroscience*, *25*(38), 8746–8754. https://doi.org/10.1523/JNEUROSCI.2809-05.2005

O'Dell, S. D., & Day, I. N. M. (1998). Molecules in focus Insulin-like growth factor II (IGF-II). *The International Journal of Biochemistry & Cell Biology*, *30*(7), 767–771. https://doi.org/10.1016/S1357-2725(98)00048-X

Pittendrigh, C. S. (1960). Circadian Rhythms and the Circadian Organization of Living Systems. *Cold Spring Harbor Symposia on Quantitative Biology*, *25*, 159–184. https://doi.org/10.1101/SQB.1960.025.01.015

Prawer, Y. D. J., Gleeson, J., De Paoli-Iseppi, R., & Clark, M. B. (2023). Pervasive effects of RNA degradation on Nanopore direct RNA sequencing. *NAR Genomics and Bioinformatics*, *5*(2), lqad060. https://doi.org/10.1093/nargab/lqad060

Quante, M., Mariani, S., Weng, J., Marinac, C. R., Kaplan, E. R., Rueschman, M., Mitchell, J. A., James, P., Hipp, J. A., Feliciano, E. M. C., Wang, R., & Redline, S. (2019). Zeitgebers and their association with rest-activity patterns. *Chronobiology International*, *36*(2), 203–213. https://doi.org/10.1080/07420528.2018.1527347

Rana, S., & Mahmood, S. (2010). Circadian rhythm and its role in malignancy. *Journal of Circadian Rhythms*, *8*(1), 3. https://doi.org/10.1186/1740-3391-8-3

Salazar, V. L., & Stoddard, P. K. (2008). Sex differences in energetic costs explain sexual dimorphism in the circadian rhythm modulation of the electrocommunication signal of the gymnotiform fish *Brachyhypopomus pinnicaudatus*. *Journal of Experimental Biology*, *211*(6), 1012–1020. https://doi.org/10.1242/jeb.014795

Sassone-Corsi, P. (2012). The Cyclic AMP Pathway. *Cold Spring Harbor Perspectives in Biology*, *4*(12), a011148. https://doi.org/10.1101/cshperspect.a011148

Silva, A., Quintana, L., Ardanaz, J. L., & Macadar, O. (2002). Environmental and hormonal influences upon EOD waveform in gymnotiform pulse fish. *Journal of Physiology-Paris*, *96*(5–6), 473–484. https://doi.org/10.1016/S0928-4257(03)00003-2

Silva, A., Quintana, L., Galeano, M., Errandonea, P., & Macadar, O. (1999). Water temperature sensitivity of EOD waveform in *Brachyhypopomus pinnicaudatus*. *Journal of Comparative Physiology A: Sensory, Neural, and Behavioral Physiology*, *185*(2), 187–197. https://doi.org/10.1007/s003590050377

Stoddard, P. K., & Markham, M. R. (2008). Signal cloaking by electric fish. *BioScience*, *58*(5), 415–425. https://doi.org/10.1641/B580508

Stoddard, P. K., Markham, M. R., Salazar, V. L., & Allee, S. (2007). Circadian rhythms in electric waveform structure and rate in the electric fish *Brachyhypopomus pinnicaudatus*. *Physiology & Behavior*, *90*(1), 11–20. https://doi.org/10.1016/j.physbeh.2006.08.013

Stoddard, P. K., & Salazar, V. L. (2011). Energetic cost of communication. *Journal of Experimental Biology*, *214*(2), 200–205. https://doi.org/10.1242/jeb.047910

Wang, T., Wang, J., Hu, X., Huang, X.-J., & Chen, G.-X. (2020). Current understanding of glucose transporter 4 expression and functional mechanisms. *World Journal of Biological Chemistry*, *11*(3), 76–98. https://doi.org/10.4331/wjbc.v11.i3.76

Zakon, H. H., Lu, Y., Zwickl, D. J., & Hillis, D. M. (2006). Sodium channel genes and the evolution of diversity in communication signals of electric fishes: Convergent molecular evolution. *Proceedings of the National Academy of Sciences of the United States of America*, *103*(10), 3675–3680. https://doi.org/10.1073/pnas.0600160103

Zakon, H. H., & Unguez, G. A. (1999). Development and regeneration of the electric organ. *Journal of Experimental Biology*, *202*(10), 1427–1434. https://doi.org/10.1242/jeb.202.10.1427

Tables

Table 1. Results of the *B. gauderio* female RNA sequencing summaries, generated using the wf-transcriptomes Netflow workflow provided by Oxford Nanopore Technologies. Read length mean and read quality for RNA sequences from each female *B. gauderio* sample.

Female		
Tank	**Read Length Mean**	**Read Quality**
B-2 Daytime	544	9
B-3 Daytime	428	9
R-2 Nighttime	441	9
R-4 Nighttime	441	9

Table 2. Results of the *B. gauderio* male RNA sequencing summaries generated using the wf-transcriptomes Netflow workflow provided by Oxford Nanopore Technologies. Shown are: A) Read length mean and read quality for each male *B. gauderio* RNA sample from this study; B) Read length mean and read quality for each male *B. gauderio* RNA sample that was sampled in the Summer of 2023.

A)

Male		
Tank	**Read Length Mean**	**Read Quality**
B-2 Daytime	631	9
B-3 Daytime	400	9
R-2 Nighttime	698	9
R-4 Nighttime	513	9

B)

Male		
Tank	**Read Length Mean**	**Read Quality**
daytime	898	10
daytime	441	8
nighttime	964	9
nighttime	585	9

Table 3. Summary of Daytime and Nighttime averages of the highest transcripts per million (TPM) for 8 male *B. gauderio* used in the analysis pipeline. Genes are categorized depending on the role they have within the EO: metabolic function, vesicle trafficking, calcium signaling, protein translation.

Gene Name	Average Daytime	Average Nighttime
Metabolic Function		
Creatine kinase M-type	768.88	1858.13
Cytochrome c oxidase subunit 5B%2C mitochondrial	2335.50	5062.00
Cytochrome b	4630.47	10968.03
Cytochrome b-c1 complex subunit 9	994.50	2006.25
Cytochrome c oxidase subunit 3	3477.25	6523.75
Cytochrome c oxidase subunit NDUFA4	1311.25	2474.75
FHIT: Bis(5'-adenosyl)-triphosphatase	156.25	1214.25
mt-atp6: ATP synthase subunit a (Fragment)	10562.75	20469.50
NADH dehydrogenase [ubiquinone] 1 alpha subcomplex subunit 2	990.50	1765.75
NADH dehydrogenase [ubiquinone] 1 alpha subcomplex subunit 6	139.00	730.25
NADH-ubiquinone oxidoreductase chain 1	4651.31	9475.13
NADH-ubiquinone oxidoreductase chain 5	5550.71	9868.88
ndufa4: Cytochrome c oxidase subunit NDUFA4	837.75	1627.88
tpi1b: Triosephosphate isomerase B	8798.75	22831.50
Vesicle Trafficking		
DYNLRB2: Dynein light chain roadblock-type 2	1478.50	775.75
Kif20a: Kinesin-like protein KIF20A	1311.25	704.25
Calcium Signaling		
Ictacalcin	7896.46	2237.25
MYOZ2: Myozenin-2	953.75	50.75
Protein Translation		
60S ribosomal protein L39	7726.25	9565.50
RPL21: 60S ribosomal protein L21	1971.00	2587.25
Rpl23: 60S ribosomal protein L23	2041.00	2764.75
rpl35: 60S ribosomal protein L35	4962.25	6266.50
rps12: 40S ribosomal protein S12	2298.00	3738.63
rps25: 40S ribosomal protein S25	6815.00	7782.50
RPS27L: 40S ribosomal protein S27-like	166.00	1302.25
rps3a: 40S ribosomal protein S3a	1122.00	1845.50
Rps9: 40S ribosomal protein S9	1081.00	1947.00

Table 4. DEGs that were statistically significant and relevant to nighttime male *B. gauderio* were categorized by the role they play within the EO: circadian core clocks, clock-controlled genes, metabolic pathways, vesicle trafficking, insulin & growth hormone signalling, endocrine metabolic regulation, other endocrine regulation and electrogenesis.

Gene Name	logFC
CIRCADIAN CORE CLOCK GENES	
CLOCK: Circadian locomoter output cycles protein kaput	3.15
CIPC: CLOCK-interacting pacemaker	2.50
ARNTL2: Aryl hydrocarbon receptor nuclear translocator-like protein 2	1.36
Cry1: Cryptochrome-1	1.77
Per1: Period circadian protein homolog 1	1.12
PER2: Period circadian protein homolog 2	1.48
PER2: Period circadian protein homolog 2	1.58
CLOCK CONTROLLED GENES	
NR1D2: REV-ERBbeta; nuclear receptor subfamily 1 Group D member 2	1.73
Nr1d2: REV-ERBbeta; nuclear receptor subfamily 1 Group D member 2	1.11
Hlf: Hepatic leukemia factor	1.36
Hlf: Hepatic leukemia factor	1.73
Hlf: Hepatic leukemia factor	1.37
Bhlhe40: Class E basic helix-loop-helix protein 40	1.75
METABOLIC PATHWAYS	
CKM: Creatine kinase M-type	1.83
mt-cyb: Cytochrome b	2.97
UQCR10: Cytochrome b-c1 complex subunit 9	2.21
mt-co3: Cytochrome c oxidase subunit 3	2.72
ndufa4: Cytochrome c oxidase subunit NDUFA4	2.42
NDUFA2: NADH dehydrogenase [ubiquinone] 1 alpha subcomplex subunit 2	2.30
MT-ND1: NADH-ubiquinone oxidoreductase chain 1	1.45
MT-ND5: NADH-ubiquinone oxidoreductase chain 5	3.72
VESICLE TRAFFICKING	
DYNLRB2: Dynein light chain roadblock-type 2	2.30
Kif20a: Kinesin-like protein KIF20A	2.40
use1: Vesicle transport protein USE1	3.33
INSULIN & GROWTH HORMONE SIGNALING	
igf2: Insulin-like growth factor II	3.91
igfbp2a: Insulin-like growth factor-binding protein 2-A	2.28
Igfbp5: Insulin-like growth factor-binding protein 5	1.02
Irs2: Insulin receptor substrate 2	1.85
Slc24a4: facilitated glucose transporter 4	3.25
Pik3cb: Phosphatidylinositol 4%2C5-bisphosphate 3-kinase catalytic subunit beta isoform	2.33
PIK3R1: Phosphatidylinositol 3-kinase regulatory subunit alpha	1.09
ENDOCRINE METABOLIC REGULATION	
LEPR: Leptin receptor	-2.36
Leprot: Leptin receptor gene-related protein	1.57
ENDOCRINE REGULATION - OTHER	
MC5R: Melanocortin receptor 5	1.26
Ar: Androgen receptor	1.36
AR: Androgen receptor (Fragment)	2.28
ELECTROGENESIS	
KCNJ11: ATP-sensitive inward rectifier potassium channel 11	2.77
scn4aa: Sodium channel protein type 4 subunit alpha	2.40
Atp1a2a: Sodium/potassium-transporting ATPase subunit alpha-2	4.87

Figures

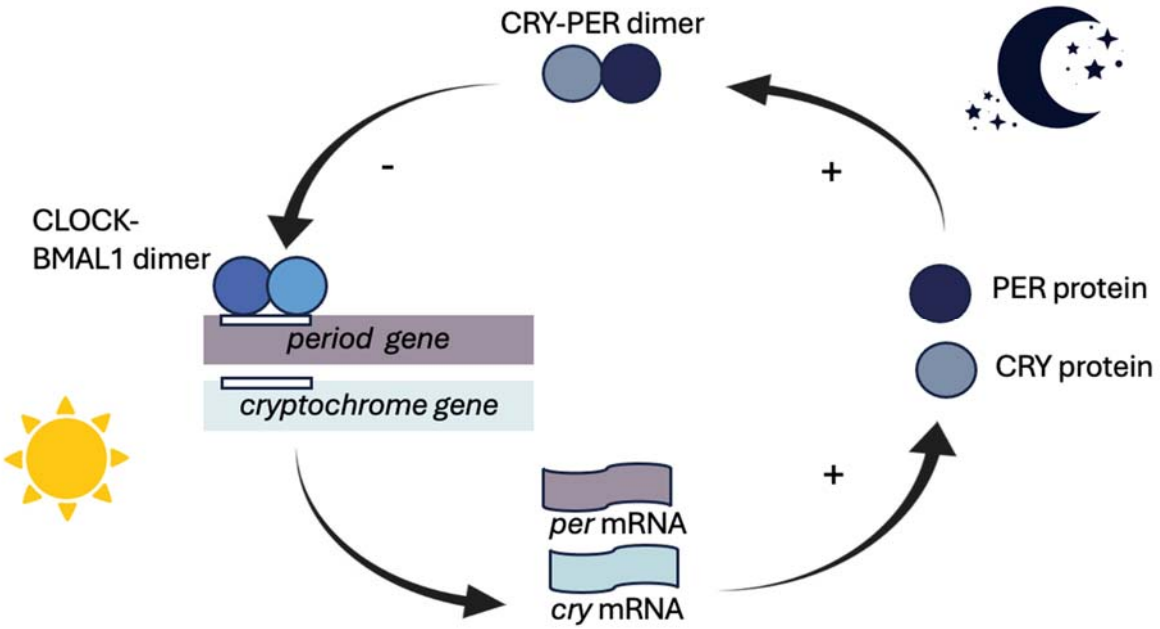

Figure 1. Simplified diagram showing the core transcriptional-translational feedback loop mechanism of the PER and CRY proteins during a 24-hour oscillation. In the early morning transcription factors BMAL1 and CLOCK bind and activate the production of PER and CRY, once PER and CRY start to accumulate in the cytoplasm they interact and form dimers. In the evening these dimers translocate into the nucleus to bind to the BMAL1-CLOCK dimer to repress their own transcription (Hall et al., n.d.; Herzog, 2007)

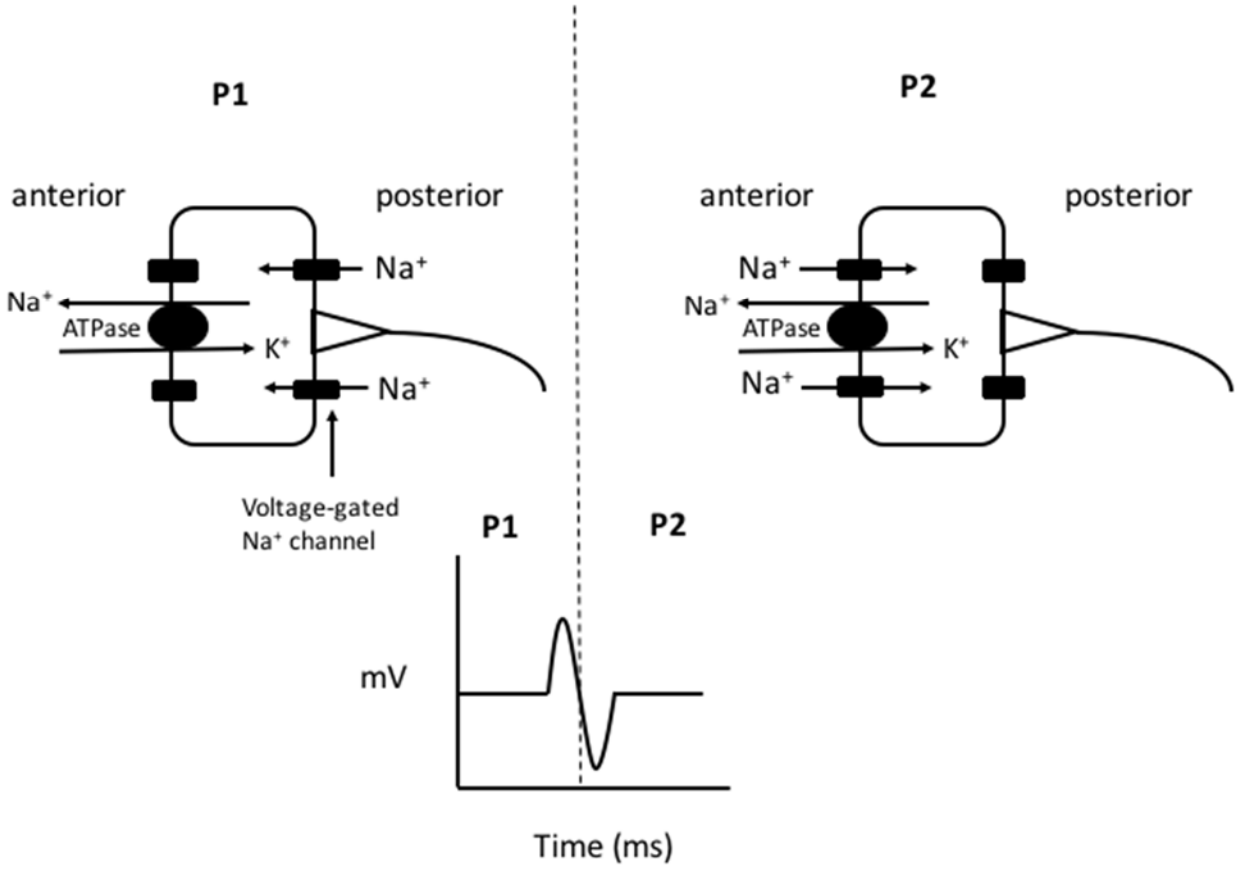

Figure 2. Simplified representation of an electrocyte during an EOD recording. The EOD of *B. gauderio* has two phases: the P1 phase (to the left of the dotted line), sodium ions enter the posterior side of the electrocyte membrane through voltage-gated sodium channels, and the P2 phase (to the right of the dotted line), in which sodium ions enter the anterior side of the electrocyte membrane through voltage-gated sodium channels. The flow of sodium ions results in the biphasic, pulse-type waveform (bottom center). The electrocyte is reset to baseline voltage by the action of the Na^+/K^+ ATPase pumps (adapted from Stoddard, 1999; Lewis *et al*., 2014).

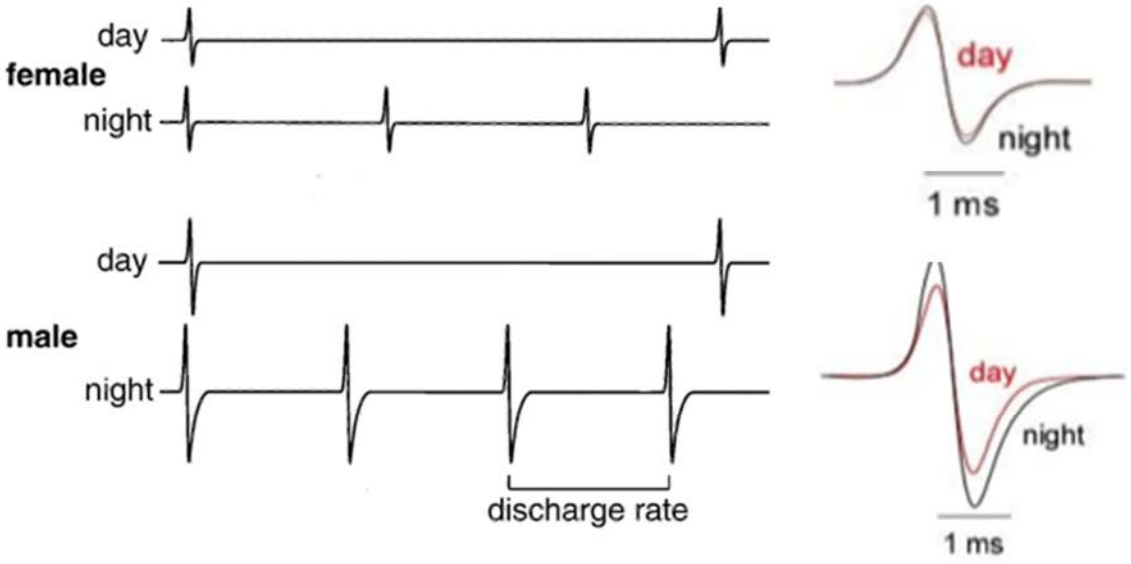

Figure 3. Illustration of the circadian regulated biphasic pulse-type waveform in both male and female. Males exhibit a larger enhancement of their EOD in relation to day-night oscillations compared to females. This includes an enhanced discharge rate, amplitude and duration (adapted from Franchina et al., 2001; Stoddard et al., 2007).

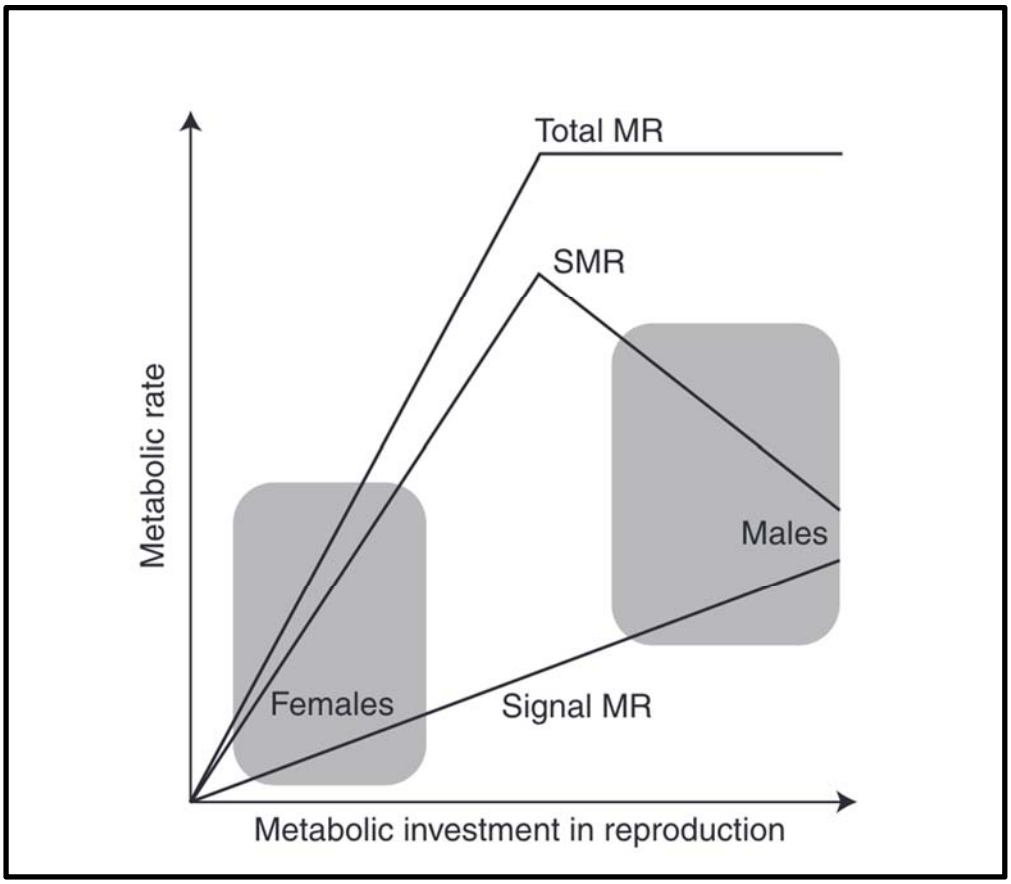

Figure 4. A line graph clearly demonstrating the inverse correlation in males between energy spent on signalling and metabolism. Whereas in female a positive correlation is seen between energy spent on signaling and metabolism (Stoddard & Salazar, 2011).

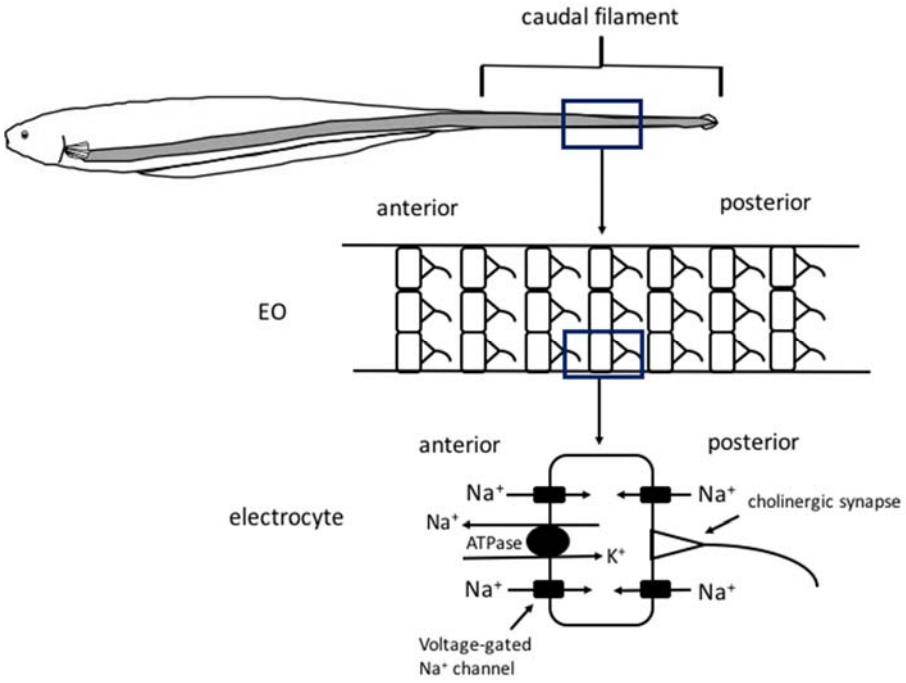

Figure 5. Representative illustrations of the electric organ (EO) of *B. gauderio* and an electrocyte. The EO of *B. gauderio* is a bilateral structure (highlighted in grey) running from the operculum to the end of the caudal filament. The EO consists of rows of electrocytes in series (middle). Each electrocyte is innervated on the posterior face at a cholinergic synapse (bottom) and contains both voltage-gated sodium channels (bottom; represented by solid black rectangles) and Na^+/K^+ ATPase pumps on the anterior and posterior faces (bottom; represented by solid black circle). Voltage-gated sodium channels allow sodium ions to enter the electrocyte and initiate an EOD. Na^+/K^+ ATPase pumps maintain the resting membrane potential (RMP) of electrocytes by pumping three sodium ions out of the cells for every two potassium ions pumped into the cells (adapted from Stoddard, 1999; Lewis *et al*., 2014).

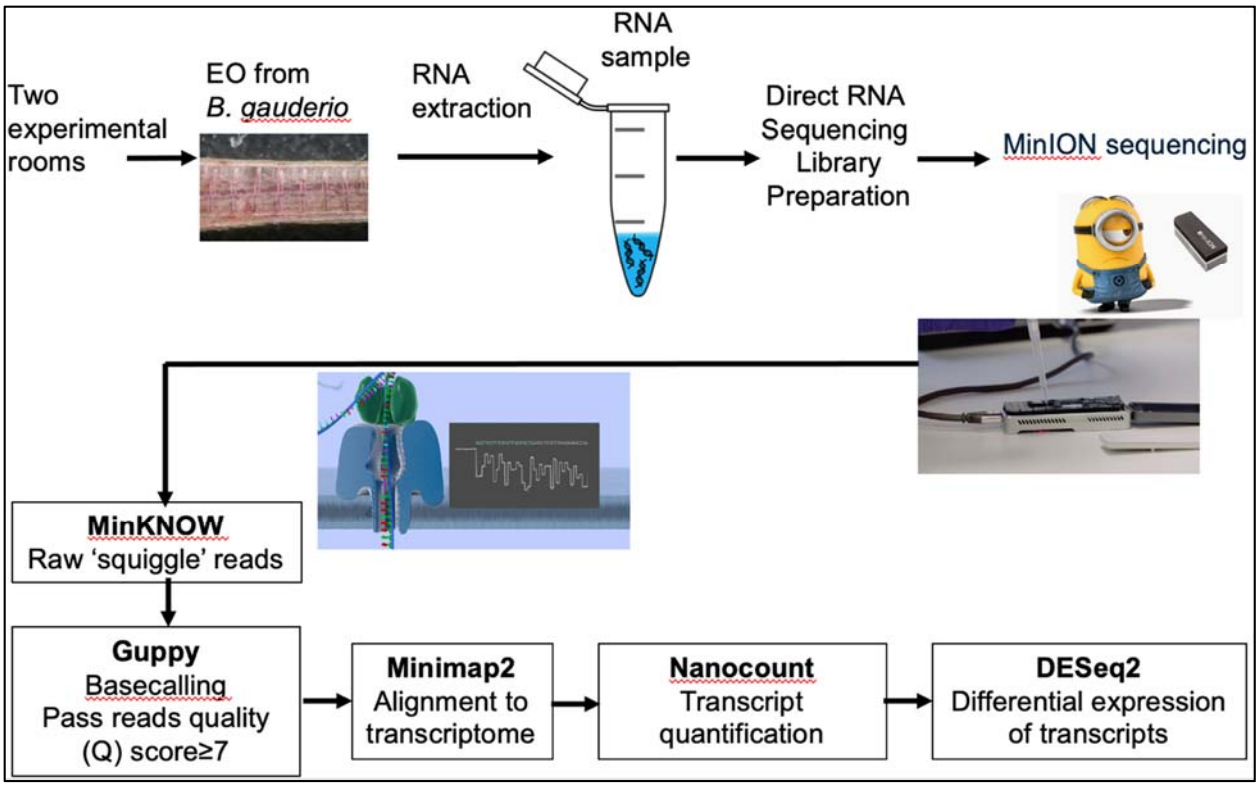

Figure 6. A schematic of the experimental methodology for my Honours Thesis project. In brief, a 1-cm segment of the electric organ (EO) will be dissected from each one of my experimental fish. This tissue will then go through RNA extraction, followed by direct RNA sequencing using the Oxford Nanopore MinION sequencer. The raw sequencing reads will be acquired using the MinKNOW software, and basecalled into nucleotide sequences by the Guppy application. Basecalled reads will be mapped to a reference *B. gauderio* transcriptome using Minimap2, and the number of transcripts will be determined using Nanocount. Differential expression of transcripts will be determined using the statistical tool DESeq2.

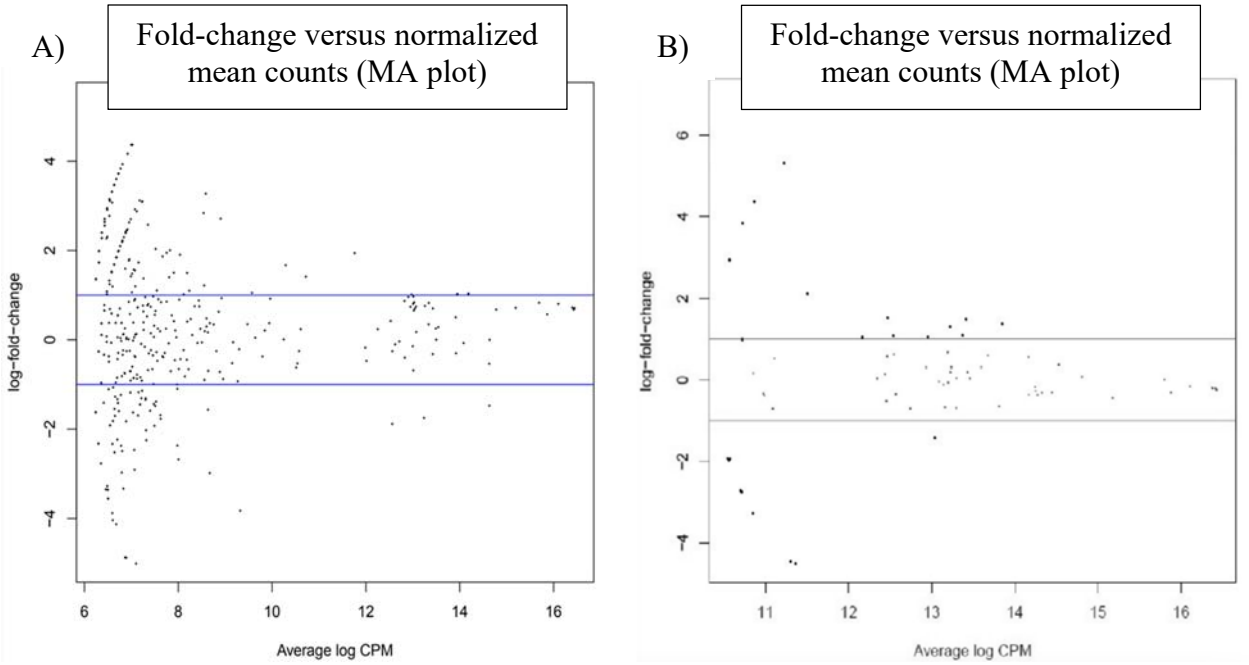

Figure 7. Log ratio (M) and mean average (A) plot of differently expressed genes. Average log CPM = average log2 counts per million; log-fold-change = expression changes between daytime and nighttime male *B. gauderio* samples. The two vertical lines indicate the up-down threshold for differential expressed genes. Values >1 represents an upregulation and <-1 represents a downregulation in nighttime gene expression relative to daytime values in A) males, and B) females *B. gauderio*.

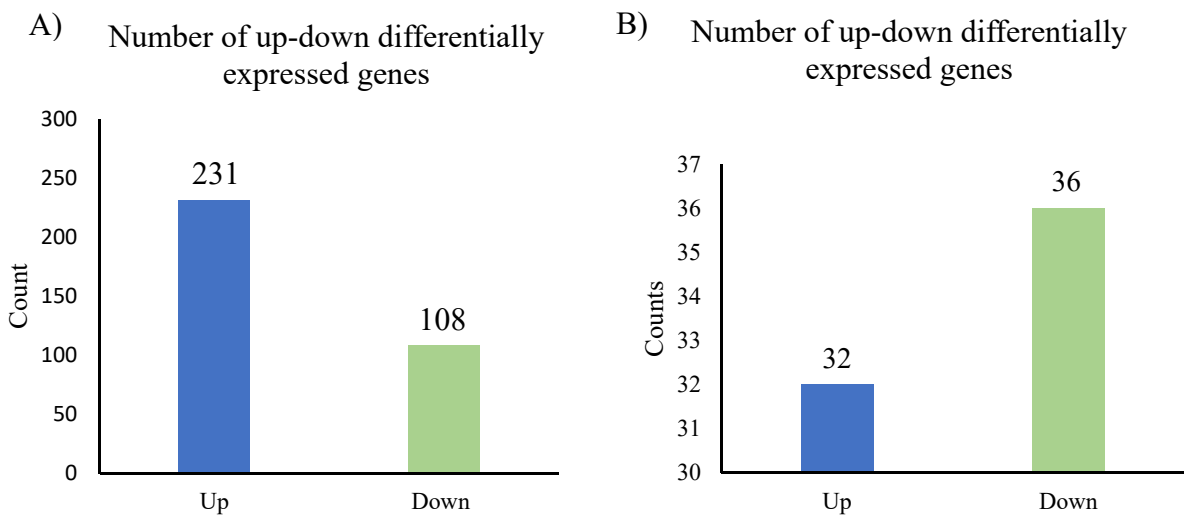

Figure 8. Bar graph of the number of upregulated and down regulated genes determined in the nighttime relative to the daytime in *B. gauderio* A) males, and B) females.

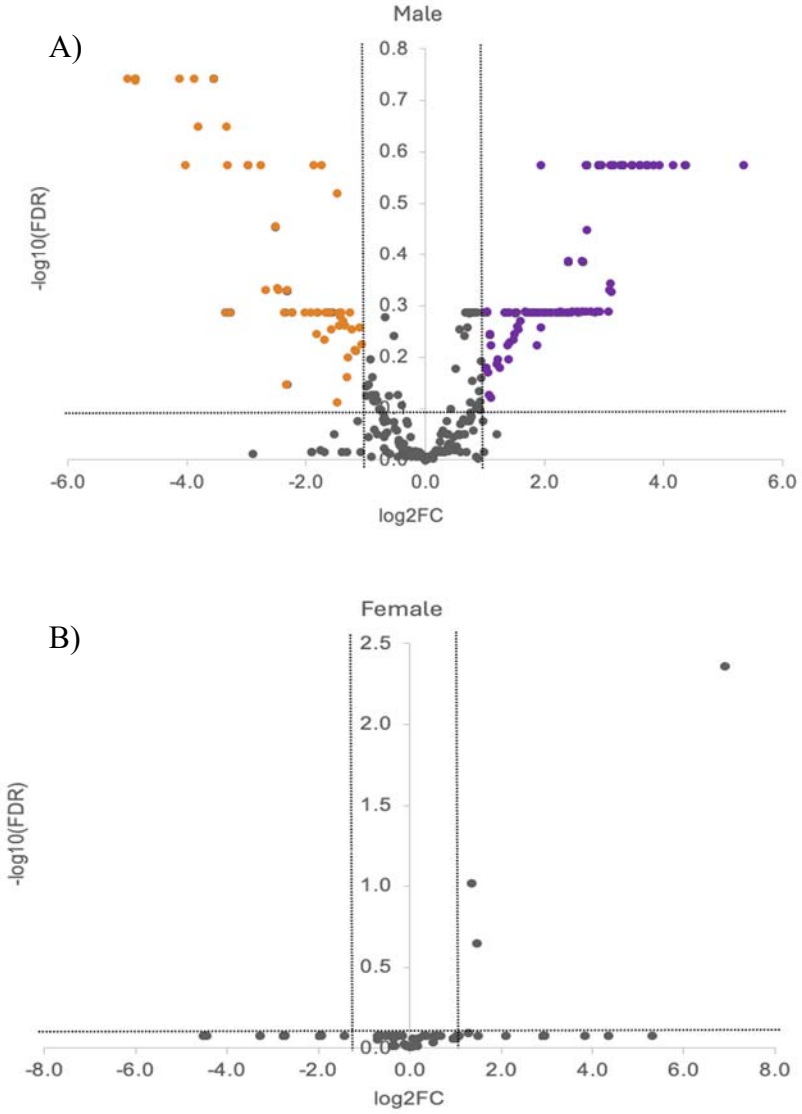

Figure 9. Volcano plots depicting -log10(FDR) values against log2(FC) in A) males and B) females *B. gauderio*. Log2(FC) values > +1 and above the 0.1 threshold for –log10(FDR) (purple dots) are DEGs that are significantly upregulated in the nighttime compared to the daytime, while log2(FC) values < -1 and above the 0.1 threshold for –log10(FDR) (orange dots) are DEGs that are downregulated in the nighttime compared to the daytime. Log2(FC) values that are between -1 and 1 and below the 0.1 threshold for –log10(FDR) (grey points) represent no significant DEGs.

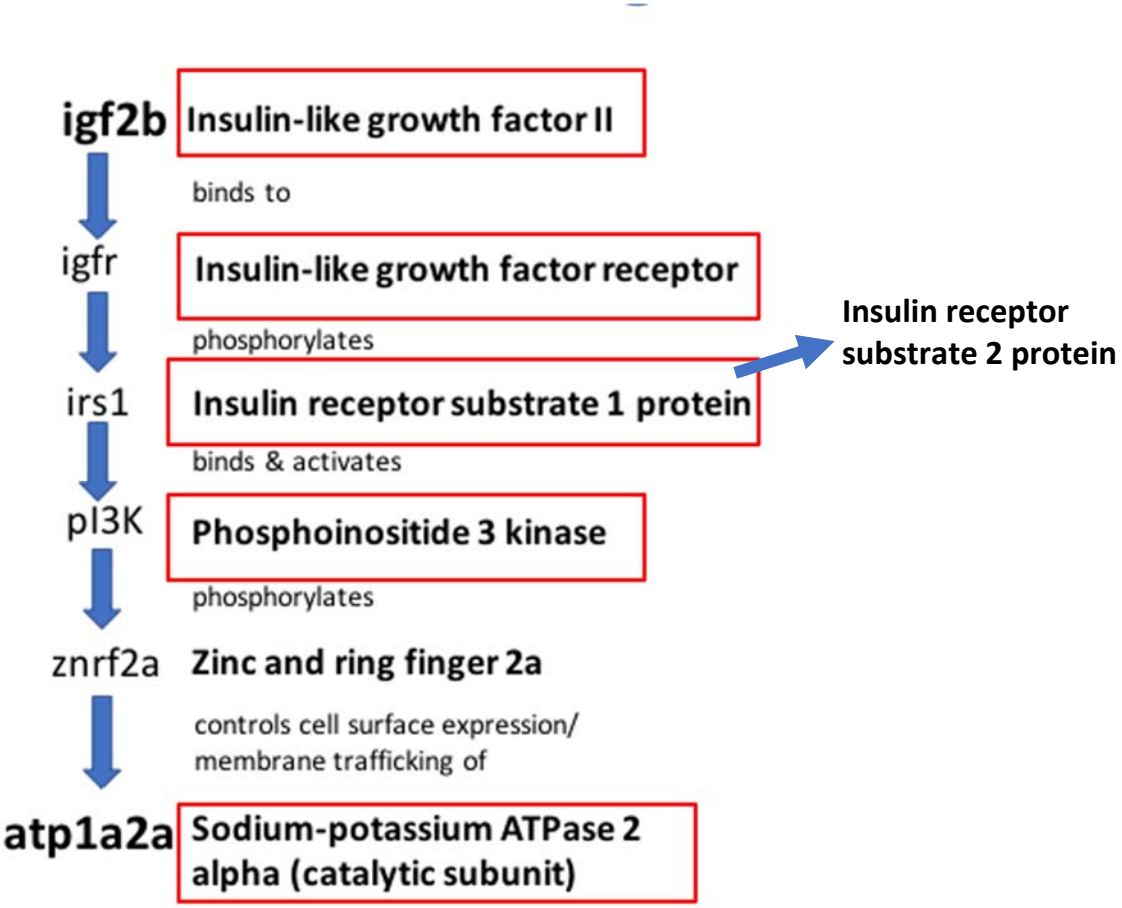

Figure 10. A schematic of the proposed cellular pathway linking the binding of IGF-II to the IGF receptor to trafficking of Na^+/K^+ ATPase pumps to the electrocyte membrane. The pathway suggests that the binding of IGF-II to the IGF receptor (IGFR) activates the insulin receptor substrate 1 protein (IRS1), which in turn activates phosphoinositide 3 kinase (PIK3), trafficking Na^+/K^+ ATPases to the electrocyte membrane. In my study the insulin receptor substrate 2 protein was upregulated (adapted from Gallant *et al*., 2014; Ivey, 2019).

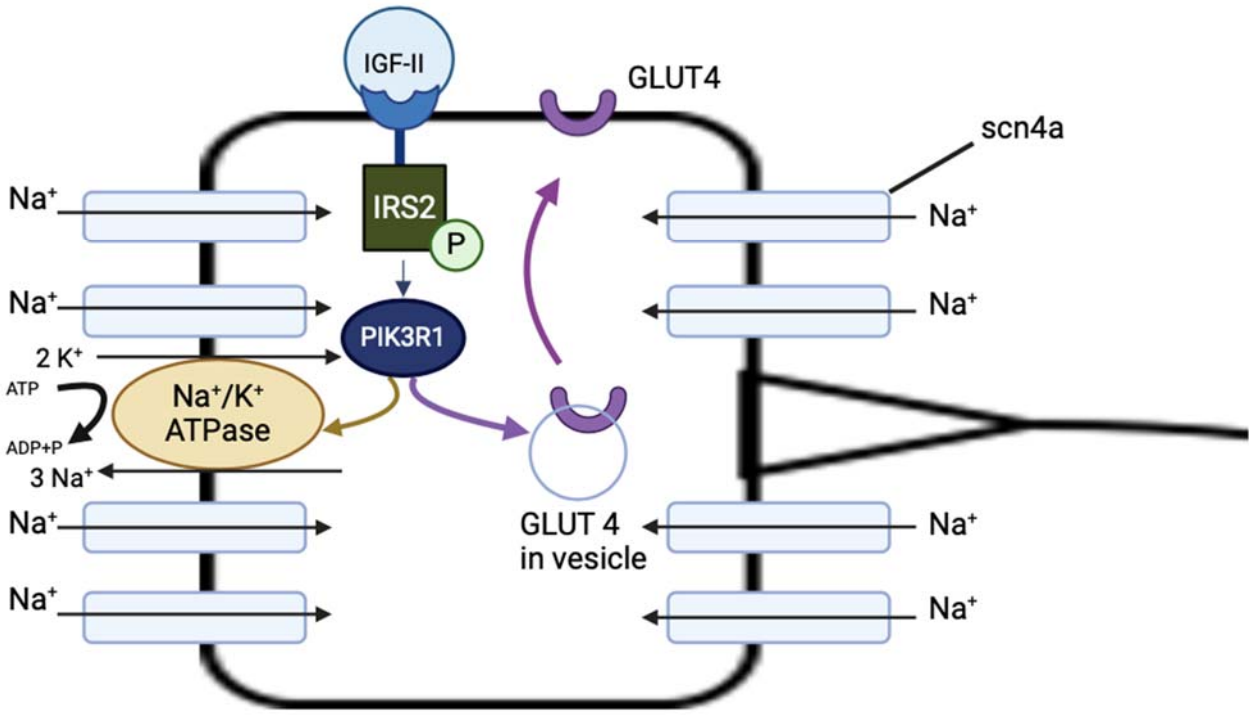

Figure 11. A schematic of a proposed cellular pathway connecting IGF-II, Na^+/K^+ ATPase, SCN4Aa, and GLUT4 in their roles in EOD modulation. The pathway suggests that the binding of IGF-II to the IGF receptor (IGFR) activates intermediate signaling molecules which result in the trafficking of Na^+/K^+ ATPase to the electrocyte membrane to reset the membrane potential from the extra Na^+ ions. The Na^+/K^+ ATPases costs energy which can be offset by the transportation of GLUT4 into the membrane for glucose uptake (adapted from Gallant *et al*., 2014; Wang et al., 2020). Voltage-gated sodium channels in the electrocyte membrane are also shown in this figure to highlight their importance in the generation of the EOD.

Appendices

Table A. NanoDrop 8000 Spectrophotometer (ThermoScientific) results for testing the purity of RNA samples. RNA samples with absorbance ratios of A260/A230 between 2.0 - 2.2 and A260/A280 between 1.8- 2.0 are considered pure.

Tank	Sex	A260/A230	A260/A280	Concentration (ng/µL)
B-2 Daytime	Male	2.19	1.84	186.50
B-2 Daytime	Female	2.25	1.89	134.80
B-3 Daytime	Male	2.19	1.90	160.40
B-3 Daytime	Female	2.25	1.93	96.49
R-2 Nighttime	Male	2.24	1.93	217.60
R-2 Nighttime	Female	2.17	1.92	158.00
R-4 Nighttime	Male	2.14	1.87	141.90
R-4 Nighttime	Female	2.22	1.88	86.20

Table B. Qubit results using the RNA IQ Assay Kit with the Qubit™ 4 Fluorometer. The RNA IQ is a value between 1-10, a lower value indicates smaller RNA fragments, a higher value indicated larger RNA fragments. B-3 Daytime female and R-4 Nighttime females have no RNA IQ values due to limitations on RNA concentration and volume.

Tank	Sex	RNA IQ
B-2 Daytime	Male	2.1
B-2 Daytime	Female	2.2
B-3 Daytime	Male	5.5
B-3 Daytime	Female	/
R-2 Nighttime	Male	2.4
R-2 Nighttime	Female	1.1
R-4 Nighttime	Male	4.5
R-4 Nighttime	Female	/

Table C. Signal recordings of sampled *B. gauderio* from four experimental groups 2 daytime females, 2 daytime males, 2 nighttime females and 2 nighttime males resulting in n=8.

Tank	Female		Male	
	Amplitude (mV)	**Duration (ms)**	**Amplitude (mV)**	**Duration (ms)**
B-2 Daytime	0.5143	0.7221	0.7872	1.3712
B-3 Daytime	0.4646	0.6208	0.8019	1.4143
R-2 Nighttime	0.8788	1.4006	1.8336	2.0533
R-4 Nighttime	0.8578	1.2985	2.0987	2.1111

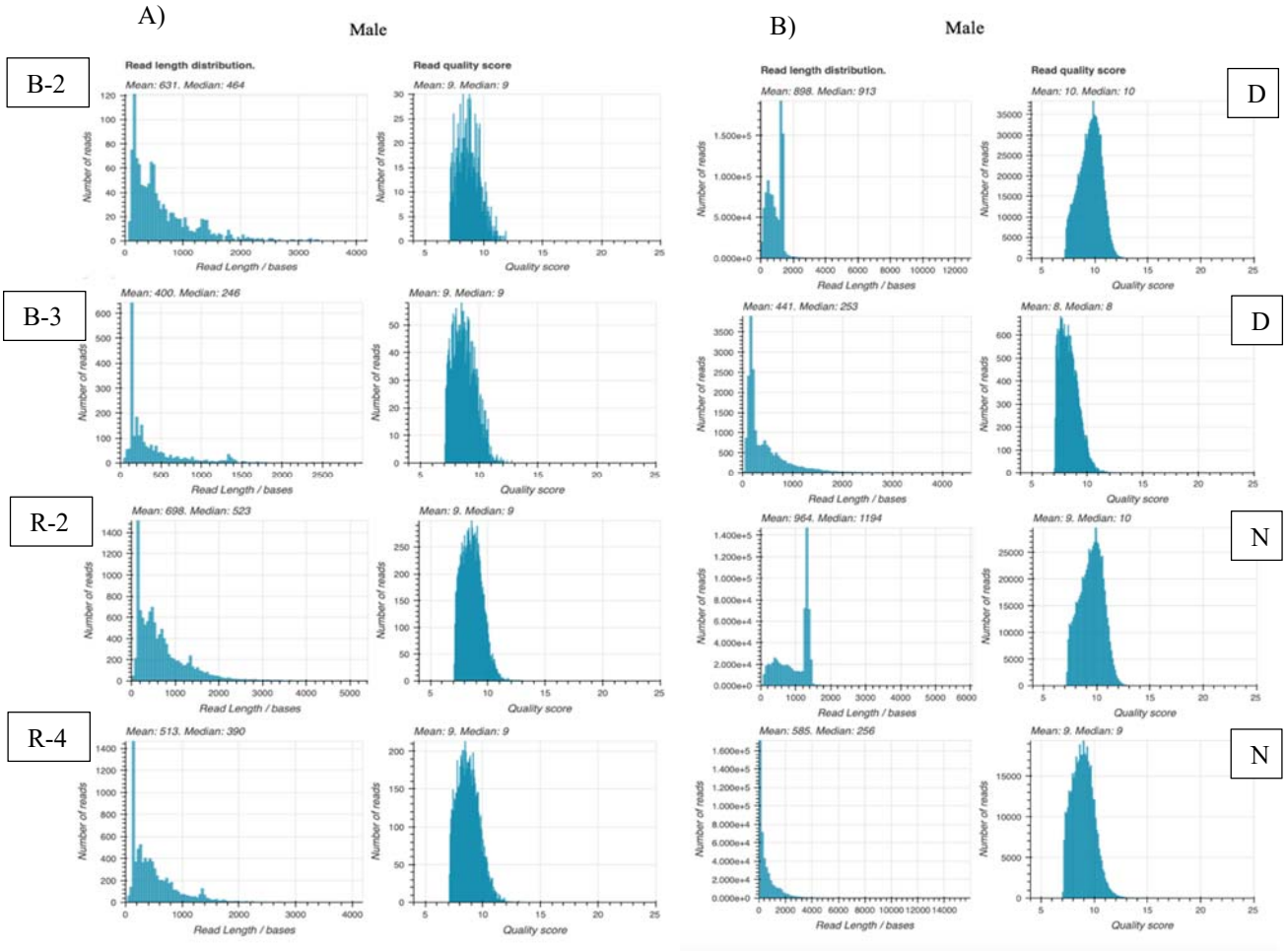

Figure A. Sequence summaries of read length distribution and read quality score for male *B. gauderio* A) sampled in 2024 for my thesis, and B) previously sampled in 2023. Results generated using the wf-transcriptomes Netflow workflow provided by Oxford Nanopore Technologies.

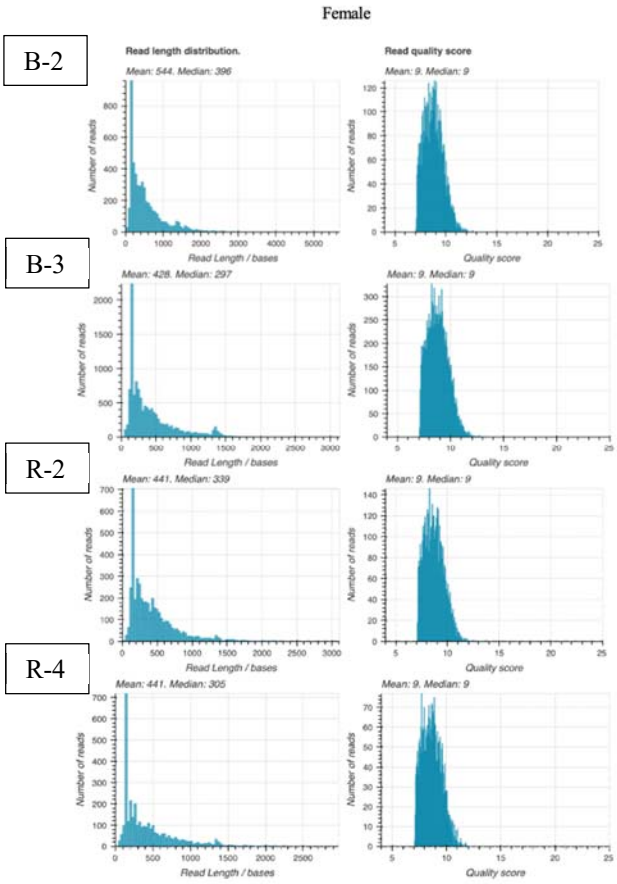

Figure B. Sequence summaries of read length distribution and read quality score for female *B. gauderio* sampled for my thesis. Results generated using the wf-transcriptomes Netflow workflow provided by Oxford Nanopore Technologies.